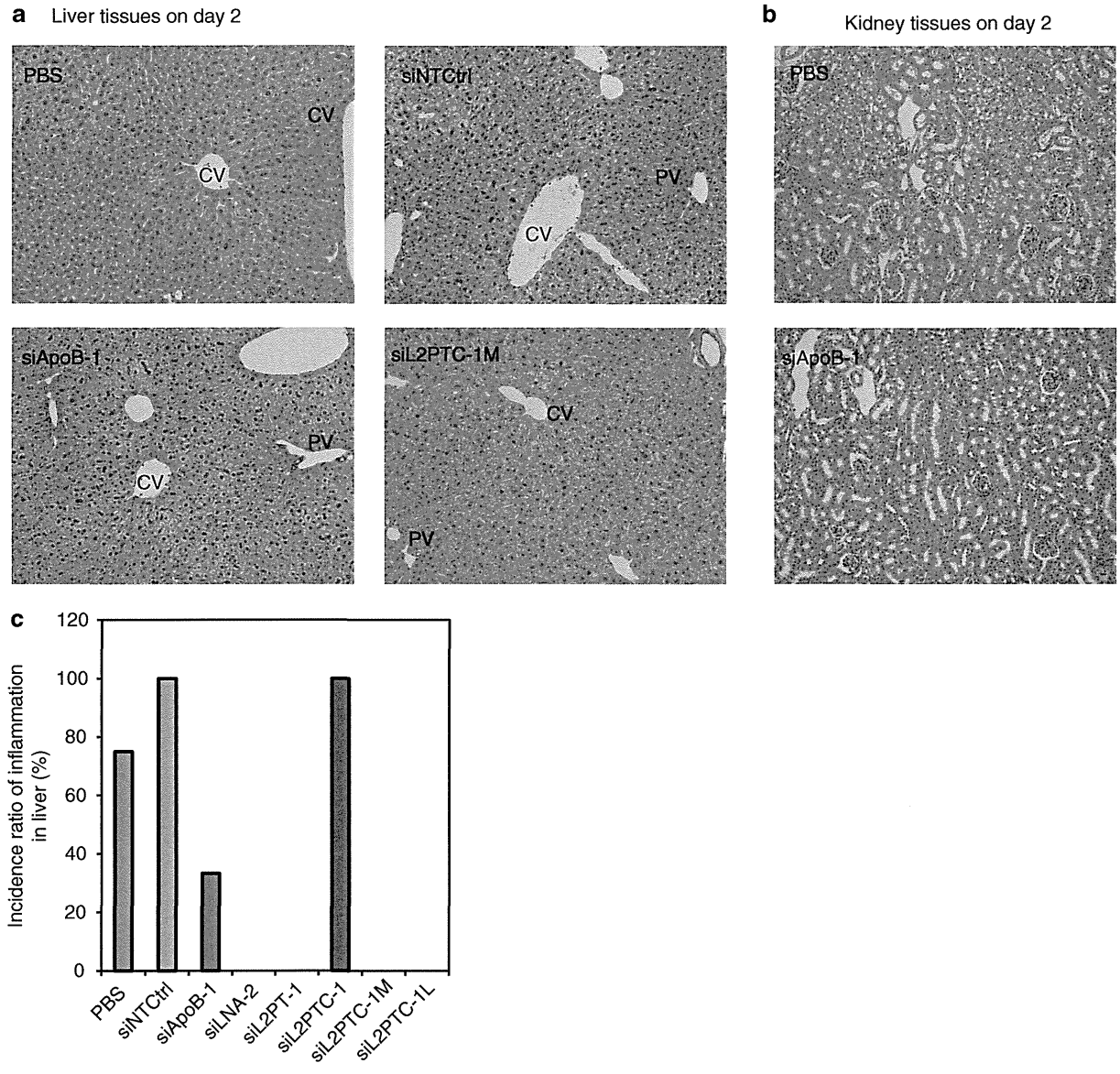

Figure 7 Liver and kidney tissue damage was assessed histopathologically using H&E staining. (**a**) Day 2 liver tissues of siNTCtrl, siApoB-1, siL2PT-1, and siL2PTC-1M were indicated as representative. (**b**) Day 2 kidney tissues of PBS and siApoB-1 were indicated as representative. (**c**) The number of mice with inflammation in the liver tissue was counted in each group, and the incidence ratio was indicated.

increases in IFIT-1 mRNA levels that were similar to those in mice receiving siL2PT-1. On day 7, continuous up-regulation of IFIT-1 expression was observed in the siLNA-2- and siL2PTC-1-treated groups. On day 2, OAS-1 expression, like IFIT-1 expression, was clearly higher in each group, except for the siL2PTC-1M- and siL2PTC-1L-treated groups, than in the PBS-treated group (**Figure 6c**). Mice receiving siApoB-1, siLNA-2, and siL2PTC-1 expressed high levels of OAS-1 mRNA on day 7 and on day 14. In contrast, neither siL2PTC-1M nor siL2PTC-1L showed significant upregulation of either gene.

Histopathological analysis for the liver and kidney

Liver and kidney tissue samples from each group were examined histopathologically. The livers of mice treated with any siRNA and PBS showed cytoplasmic vacuolation throughout the experiment. Furthermore, centrilobular hypertrophy of the liver was evident in a majority of the groups with the exception of the PBS- and siL2PTC-1M-treated groups on day 2 (**Figure 7a**). However, these lesions were seen in samples from every group on day 14. On day 14, inflammatory lesions were observed in mice treated with PBS, siNTCtrl or siApoB-1, and also in mice treated with siL2PTC-1 on day 24. In addition, slight granuloma or focal necrosis was sporadically seen. In contrast, no evidence of any toxicological effect was found in kidneys from any of the mice at any point in the experiment (**Figure 7b**). On day 24, we counted the mice in each group that exhibited liver inflammation (**Figure 7c**). Some mice in the PBS-, siNTCtrl-, siApoB-1-, and siL2PTC-1-treated groups showed inflammation in the liver, whereas

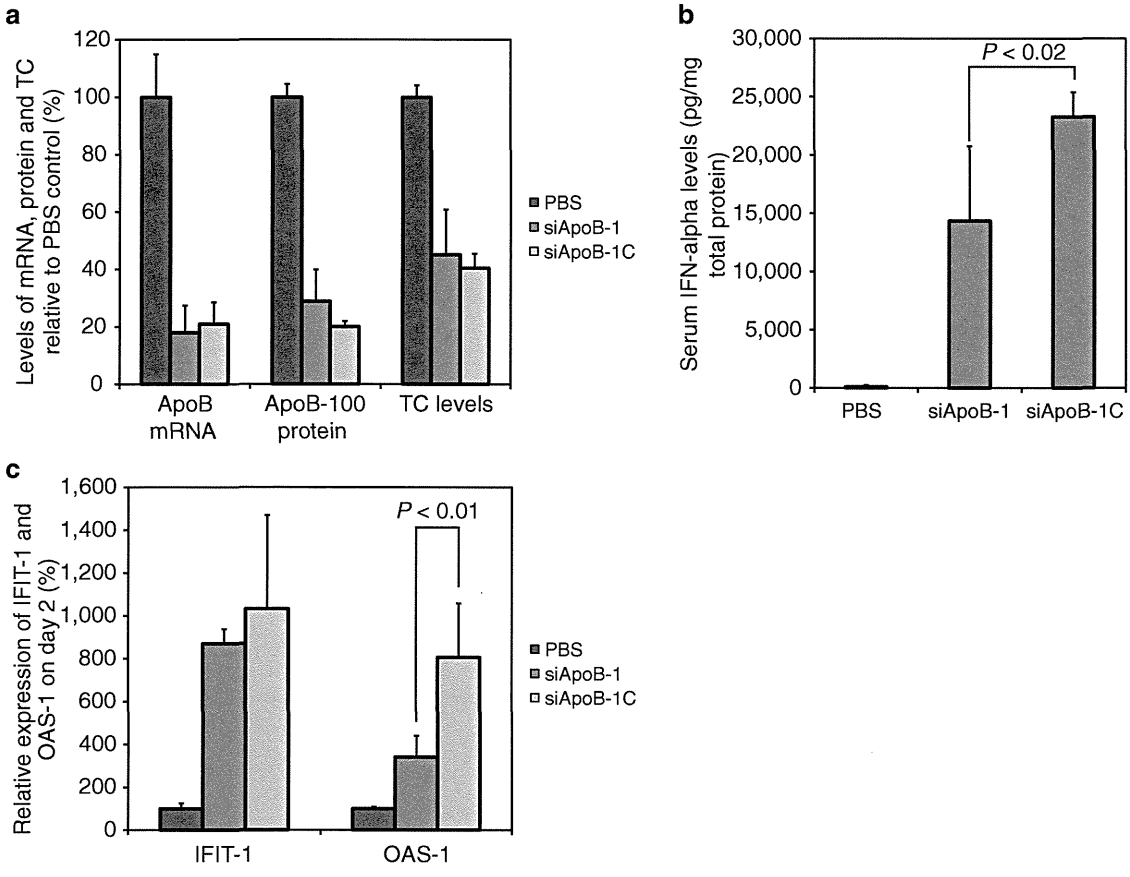

Figure 8 Pharmacological parameters and innate immune responses 2 days after the injection of siApoB-1C or siApoB-1. (**a**) ApoB mRNA inhibition, apoB-100 protein levels in the liver, and serum TC levels were measured 2 days after the injections. (**b**) IFN-α levels in serum 6 hours after injection of siApoB-1 and siApoB-1C. (**c**) Comparison of the effects of siApoB-1 and siApoB-1C on IFN-α-related gene expression. IFIT-1 and OAS-1 mRNA expression was normalized to GAPDH expression. All values are the means ± SD of three to four animals.

none of the mice in any other groups showed evidence of liver inflammation.

Cholesterol-conjugated siApoB-1 induced slightly high levels of IFN-α and its related gene expression compared with siApoB-1

Cholesterol-conjugated siL2PTC-1 not only abbreviated the duration of pharmacological parameters but also induced sustained high expression of IFN-α-related genes such as *IFIT-1* and *OAS-1* (**Figures 4c** and **6b,c**). Only mice receiving siL2PTC-1 exhibited inflammation in the liver on day 24; there was no inflammation in any mouse receiving other modified siRNAs. We hypothesized that cholesterol conjugation may have facilitated the interaction between the siRNA and some proteins that play an important role in evoking the innate immune response. We designed cholesterol-conjugated siApoB-1 (siApoB-1C; **Table 1**) to assess the impact of this modification on immune response, and used siApoB-1 as a control. Mice were injected with 5 mg/kg of siApoB-1C formulated with Invivofectamine 2.0 reagent via the tail vein and sacrificed 2 days after injection. Blood samples were collected from the tail vein at 6 hours after injection to measure the serum IFN-α concentration. Mice treated with siApoB-1C exhibited overt body weight loss of up to 11% on days 1 and 2. On day 2, the values of three pharmacological parameters (apoB mRNA, apoB-100 protein levels and serum TC levels) were similar in animals receiving siApoB-1C and those receiving siApoB-1 (**Figure 8a**). IFN-α induction in mice receiving siApoB-1C was significantly higher than that in mice receiving siApoB-1 ($P < 0.02$) (**Figure 8b**). Interestingly, IFIT-1 mRNA levels were similar in the siApoB-1C-treated group and the siApoB-1-treated group, but OAS-1 mRNA levels were twofold higher in the siApoB-1C-treated group than in the siApoB-1-treated group ($P < 0.01$) (**Figure 8c**).

The siL2PT-1M induced an efficient reduction of pharmacological parameters without any induction of IFN-α or upregulation of IFN-α-related gene expression

Based on these *in vivo* analyses and previous work by Judge *et al.*, we designed siL2PT-1M, which had additional 2′-OMe modifications in the immunostimulatory motif, as well as siL2PTC-1M, to completely eliminate the immune response;[32] siL2PT-1M, like siL2PT-1, was designed to be effective for apoB lowering. Mice were injected with 5 mg/kg of siL2PT-1M formulated with Invivofectamine 2.0 reagent via the tail vein and sacrificed on day 2 or 24. No remarkable reduction of body weight was observed in the siL2PT-1M-treated group compared with the PBS-treated group. The RNAi effect

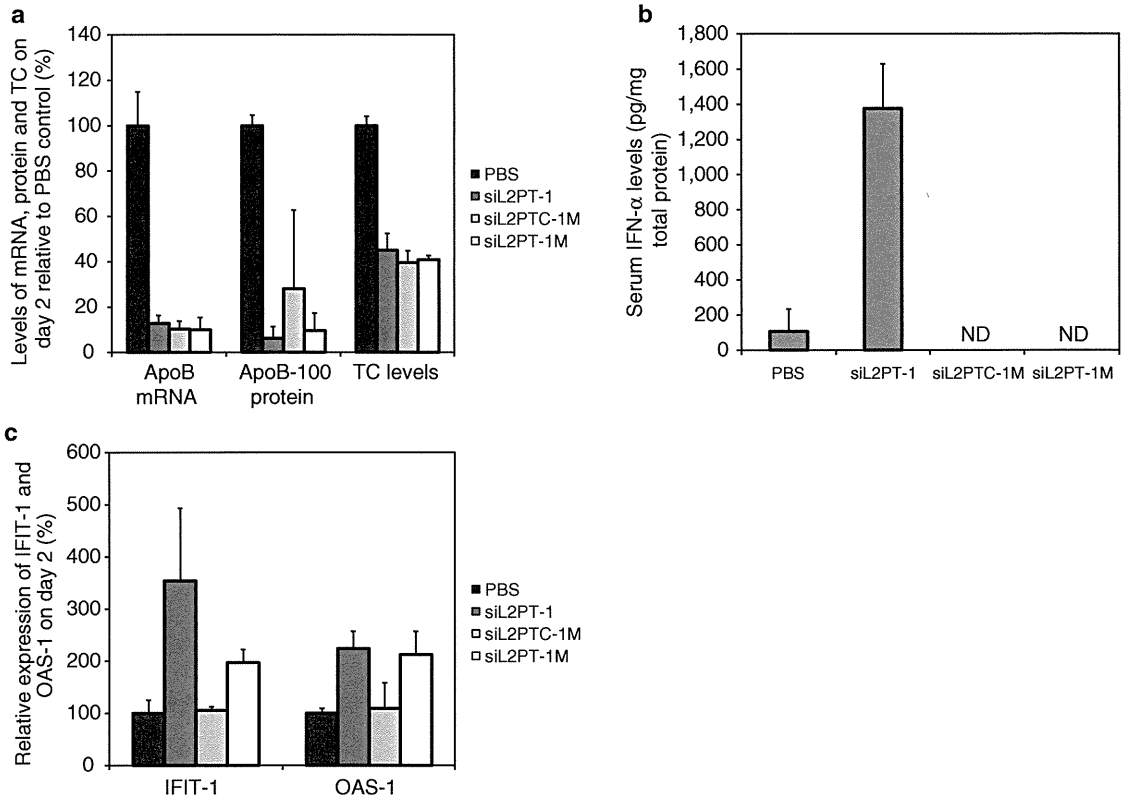

Figure 9 Comparison between siL2PT-1-, siL2PTC-1M-, and siL2PT-1M-mediated effects on pharmacological parameters and immune responses on day 2. (**a**) ApoB mRNA inhibition, apoB-100 protein levels in the liver, and serum TC levels were all measured 2 days after the injection of the siRNAs. (**b**) IFN-α levels in serum 6 hours after injection of each siRNA. (**c**) Comparison of the effects of siL2PT-1, siL2PTC-1M and siL2PT-1M on IFN-α-related gene expression. IFIT-1 and OAS-1 mRNA expression was normalized to GAPDH expression. All values are the means ± SD of three to four animals.

of siL2PT-1M was up to >90% on day 2, and thus was similar to that of siL2PT-1 (**Figure 9a**). On day 2, the serum TC levels of the siL2PT-1M-treated group showed a significant reduction of up to 60% as well as that of the siL2PT-1-treated group. This effective serum TC lowering lasted until day 24, and then, the serum TC levels were similar to those in mice receiving siL2PTC-1M. Although the IFIT-1 and OAS-1 mRNA expressions were slightly higher in the siL2PT-1M-treated group than in the PBS-treated group, serum IFN-α was not detected in the siL2PT-1M-treated group as well as in the siL2PTC-1M-treated group (**Figure 9b,c**).

Discussion

First, we designed two types of 2′,4′-BNA/LNA-modified siRNAs to avoid the undesired incorporation of sense strand with RISC and to give it nuclease resistance. Although siLNA-1 has been hypothesized to be more active than siLNA-2 *in vitro*, since the key property in strand bias was proven to be thermodynamic stability of different region (5′ or 3′-side) of duplex, siLNA-2 had a lower IC_{50} value and a much higher nuclease resistance than siLNA-1 (**Figures 1b** and **2b**).[26,35–37] However, incorporation of 2′,4′-BNA/LNA in the immunostimulatory motif (as represented by siL2PTC-1L) abolished not only the immune reaction but also the RNAi effect due to unrecognizable nucleic acids in the position related to the RNAi machinery (**Figure 4c**). Our results crucially suggested that 2′,4′-BNA/LNA modifications should be used in the sense strand as nuclease resistance and regulation of strand bias, but not in the site related to RISC formation including pre-cleavage of sense strand and RISC-mediated cleavage of target RNA.

To the best of our knowledge, no study has attempted to comprehensively assess the effects caused by 2′,4′-BNA/LNA-modified siRNAs combined with other artificial nucleic acids *in vivo*. Our siRNAs that were based on siLNA-2 and had additional modifications exhibited various effects both *in vitro* and *in vivo*. The RNAi effects of siL2PT-1, which had additional PS modifications, persisted longest with slightly inhibited IFN-α production compared with that of siLNA-2 (**Figures 4c** and **6a**). These findings indicated that it is possible to eliminate the innate immune response when the PS modifications are in appropriate positions within siRNA. Previously, Judge *et al.* reported that although modification of all cytidine residues with 2′-OMe in the sense strand of an siRNA that had the same sequence in our study evoked immune response, modification of all adenosine residues in the sense strand almost inhibited the IFN-α induction. And modification of all uridine or all guanosin in the sense strand of siRNA completely abrogated the immune response. These findings indicated that modification of the sense strand alone

could eliminate the immune reactions in any siRNAs and that uridine and guanosine were directly related to the induction of an innate immune response, and partial adenosine also related to immune response.[32] In our study, the slightly diminished IFN-α levels associated with siL2PT-1 (**Figure 6a**) were attributed to partial adenosine modification in the 5′-CACAC-3′ motif, which is complementary to the immunostimulatory motif. Taken together, our results and those of Judge *et al.* indicated that modifying the adenosine residues complementary to the immunostimulatory motif and 5′-UG-3′ (tenth from the 5′-end) in a sense strand results in elimination of innate immune response with only sense strand chemical modification in this sequence. Although, in this sequence, 5′-UG-3′ is in the position related to pre-cleavage of the sense strand, 2′-OMe modification at this site was proven to be well tolerated by the RNAi mechanism.[38,39]

Cholesterol conjugation has been widely used as a delivery vehicle for naked siRNA and nuclease resistance.[25,40,41] We hypothesized that cholesterol conjugation of siRNA would lower the recognition of nucleases and alleviate the recognition of innate immune systems due to its slight bulky structure at the 3′-end.[31] Unexpectedly, cholesterol conjugation resulted in a markedly reduced RT_{50} of mRNA inhibition and slightly enhanced immune reactions (**Figures 4a,c** and **6b,c**). Although a similar RNAi effect was observed on day 2 between the siL2PTC-1- and siL2PT-1-treated groups in the *in vivo* experiment (**Figure 4c**), these effects were attributed to saturation of the RISC complex due to excessive concentrations of siRNA in the liver cell.[42] The factors that affect the duration of pharmacological effects are the disappearance rate of siRNA and turnover rate of active RISC in the cell. Although the cholesterol conjugation in the sense strand wields an influence on the RNAi effect via RISC formation under the conditions of a low concentration of siRNA (**Figure 3a**), the stability of siRNA against enzymatic degradation has an impact on the sustained RNAi effect when the siRNA is in excess in the cell, as was the case in our *in vivo* experiment. In the RNase T experiment, the stability of siL2PTC-1 was comparable to that of siL2PT-1, although the image of siL2PTC-1 indicated partial degradation of siL-2PTC-1 (**Supplementary Figure S3 and Supplementary Materials and Methods**). This partially degraded moiety was considered to be cholesteryl-TEG, because the bands after 0 hour showed a molecular weight similar to those of siL2PT-1. According to previous work conducted by Haley *et al.*, the turnover rate of active RISC complexes containing the antisense strand that was the same sequence between siL2PT-1 and siL2PTC-1 would be comparable.[42] Namely, it was suggested that cholesterol conjugation might slightly alter the disappearance rate of siRNA in the cell, except for consumption by RISC formation. IFN-α levels of siL2PT-1 and siL2PTC-1 were comparable and cholesterol-conjugation did not alter the innate immune response (**Figure 6a–c**). However, interestingly, cholesterol-conjugated siApoB-1 enhanced IFN-α production compared with nonmodified siApoB-1 (**Figure 8b**). Therefore, the mechanism by which cholesterol-conjugation provokes an immune reaction may have an impact on the disappearance rate of siRNA. Indeed, siL2PTC-1M having a 2′-OMe-modified immunostimulatory motif showed slightly better duration of pharmacological parameters than those of siL2PTC-1 (**Figure 4b–d**). Primary recognition of siRNAs is evoked by TLR7, which is located in the endosomal compartment.[33] In the cytosol, retinoic acid-inducible gene-I (RIG-I) acts as a sensor of viral RNA via binding and was activated by single-strand RNA or double-strand RNA containing 5′-triphosphates or blunt-ended siRNA.[43,44] Although RIG-I induces type-I IFNs by recognizing viral RNA, their mRNA expression is affected by IFN-α from other signal pathways.[44] RIG-I mRNA expression in the mice receiving siL2PT-1 or siL2PTC-1 was slightly higher than that in mice receiving PBS (**Supplementary Figure S4**), and in each group, RIG-I mRNA expression was slightly correlated with serum IFN-α levels, indicating that slightly elevated levels of RIG-I mRNA were attributed to the response to IFN-α. Therefore, the facilitation of the immune response by cholesterol conjugation might happen in the endosome. There are three possible hypotheses. (i) Cholesterol-conjugated siRNA binds more strongly to proteins in serum or cytosol than does normal siRNA.[25,45] The cholesterol moiety may hydrophobically interact with some sort of protein (proteins on an endosomal membrane, such as TLRs, which have a hydrophobic leucine-rich repeat) or endosomal membranes, resulting in facilitating the interaction between siRNA and TLR. Then the aberrant siRNA-protein complex is metabolized from the cell, which leads to early lowering of the level of siRNA in the cell. (ii) Due to the strong affinity between cholesterol and delivery vehicle used in this study, cholesterol-conjugated siRNA cannot readily escape from delivery vehicles, resulting in generation of the aberrant complex, and the complex was metabolized. (iii) Due to the hydrophobicity of the cholesteryl-TEG group, cholesterol-conjugated siRNAs or precleavage debris of the sense strand containing a cholesteryl-TEG moiety could form micelles or be aggregated in the cell. This aberrant complex induces cytotoxic effects.

Our results indicated that using the cholesterol-conjugated siRNA with the lipid carrier resulted in not only shortened duration of pharmacological parameters, but also an enhanced immune response. The cholesteryl-TEG group of cholesterol-conjugated siRNA was immediately eliminated in the RNase T solution (**Supplementary Figure S3**). We measured mRNA levels of SREBP2 (a transcriptional activator required for lipid homeostasis) and ACAT1 (an enzyme which esterifies the free cholesterol and stores cholesteryl esters in lipid droplets) on day 2 in the siApoB-1C- and siApoB-1-, and PBS-treated groups (**Supplementary Figure S5**). There was no significant difference in these mRNA levels among the groups, indicating that the cholesterol synthesis and conservation system were not influenced by precleavage debris of the cholesteryl-TEG group of siRNA or by silencing the apoB mRNA.

Based on the histopathological analyses and serum chemistry, the siRNA-carrier complex used in this study caused almost no nephrotoxic effects. In contrast, some siRNAs (siApoB-1, siLNA-2, siL2PTC-1, siApoB-1C, and siNTCtrl) cause serious liver damage. Although siRNAs which induced IFN-α were also associated with elevation of serum AST levels on day 2, there was no correlation between IFN-α concentration and serum AST levels. However, the elevated AST levels on day 2 and centrilobular hypertrophy were highly associated findings. The siRNAs with chemical modifications in the immunostimulatory motif exhibited normal range

in centrilobular hypertrophy, claiming the needs for complete elimination of the immune response by an siRNA. Mice exhibiting the IFN-α production exhibited overt up-regulation of CYP7α1 (the first and rate-limiting enzyme in bile acid synthesis) mRNA on day 2, indicating that cholesterol was converted to bile acid at high rates in the cells (**Supplementary Figure S6**). We also found an association between the increases in ALT levels and inflammatory lesions on day 24 in PBS-, siNTCtrl- and siL2PTC-1-treated mice, but not in siApoB-1-treated mice. The inflammation and increased ALT levels in the PBS-treated group were attributed to deposition of fat in the liver caused by the atherogenic diet. Almost all mice receiving an siRNA targeting apoB mRNA showed no incidence of inflammation in the liver on day 24 but not in mice receiving siApoB-1 or siL2PTC-1 (**Figure 7c**), indicating that translational restriction of apoB may be involved in chronic liver toxicity in mice fed an atherogenic-diet.

This is the first report to show comprehensive effects by 2′,4′-BNA/LNA-modified siRNA combined with other artificial nucleic acids *in vivo*. In this article, we demonstrated that each siRNA that was designed based on siLNA-2 significantly reduced the apoB mRNA levels in liver and serum TC levels. In particular, siL2PT-1M-mediated sustained duration of the RNAi effect and other pharmacological parameters, but did not induce IFN-α. In cases of dyslipidemia, including homozygous familial hypercholesterolemia, apoB is an attractive drug target for LDL-lowering therapy because inhibition of apoB-100 directly downregulates the generation of LDL particles. Our results have much importance for the development of apoB-lowering siRNA medicines. Importantly, our findings on immunostimulation by immunostimulatory siRNA (isRNA) raise a question about the use of cholesterol-conjugated isRNA with lipidic or cationic delivery vehicles. It was also suggested that modifying the adenosine residues complementary to the immunostimulatory motif and 5′-UG-3′ (tenth from the 5′-end) in the sense strand result in elimination of the innate immune response with chemical modification only in the sense strand. If we were able to alter the nuclease resistance and to abrogate the immunostimulation of potential siRNAs by chemical modification of only the sense strand, many siRNA candidates that have been rejected without any analyses would be reassessed and analyzed, and these changes could lead to the development of more efficient siRNA drugs. Our analyses of the effects of chemical modification in siRNAs on pharmacological parameters, tissue toxicity and innate immune response may contribute in important ways to the development and design of siRNA drugs for various genetic or chronic disorders.

Materials and methods

Design of siRNAs. The siRNAs used in this study consisted of 23-nucleotide sense and antisense strands. The targeted site in apoB mRNA was chosen based on the study conducted by Soutchek *et al.*[25] We also prepared an siRNA consisting of 21-nucleotide sense and antisense strands as a control siRNA (siNTCtrl). This sequence was previously reported as a nontargeting control sequence that contains at least four mismatches to any human, mouse or rat gene.[46] All sequences and modifications of siRNA are listed in **Table 1**. All siRNAs were chemically synthesized by GeneDesign (Ibaraki, Japan) and were received as desalted. Equimolar concentrations of each sense and antisense strand were incubated at 95 °C for 5 minutes in RNase/DNase free water and then cooled slowly at room temperature for 12 hours.

UV melting experiment. We measured the T_m value of each siRNA by conducting UV melting experiments with a Beckman DU-650 spectrometer including a T_m analysis accessory. Annealed siRNAs were dissolved in 10 mmol/l sodium phosphate buffer (pH 7.2) containing 100 mmol/l NaCl to a final concentration of 1 μmol/l. The melting profiles at temperatures ranging from 25°C to 95 °C were recorded at 260 nm using a scan rate of 0.5 °C/min. The melting temperature (T_m) was calculated as the temperature at which the duplexes were half dissociated and each T_m was determined by taking the first derivative of the melting curve.

Serum stability. To determine the stability of siRNAs in serum, each siRNA (final concentration of 0.5 μmol/l) was incubated in a sample of 100% mouse serum at 37 °C. We measured the amount of intact siRNA that remained in the serum at defined time points. Specifically, we took a 5-μl sample from each serum-siRNA mixture at 0 minute, 30 minutes, 60, 120, 360, 720, 1,440, and 2,880 minutes. Each 5-μl sample was diluted with 5 μl of three times TBE buffer (final concentration: 50 mmol/l THAM (Tris(hydroxymethyl)aminomethane), 48.5 mmol/l borate, 2 mmol/l EDTA, pH 8.2) and 5 μl of distilled water and then frozen in liquid nitrogen. Denatured siRNA was prepared by incubating double-strand siRNA at 95 °C for 5 minutes and immediately cooled at 4 °C. These 15 μl of samples and 10 bp DNA step ladder (Invitrogen) were then subjected to electrophoresis on 20% TBE gel (Invitrogen) for 110 minutes at 120 V. RNA bands were visualized by using SYBR Gold (Invitrogen). Gel images were taken with LAS-4000 mini image analyzer (FUJIFILM, Tokyo, Japan) and the intensity of bands was measured by using Image J software (http://rsbweb.nih.gov/ij/) freely available on the Internet.

Cell culture and transfection of siRNAs. To evaluate the gene-silencing ability of individual siRNAs *in vitro*, we used a mouse hepatic cell line, NMuLi. The cells were seeded in 9.62 cm^2 6-well plates at 5×10^5 cells/well in DMEM (GIBCO, Grand Island, NY) containing 10% fetal bovine serum and 1% penicillin/streptomycin (Gibco) and incubated for 24 hours under 5% CO_2 at 37 °C. After incubation, the culture medium was replaced with antibiotic-free DMEM. Each siRNA, at several different concentrations, was transfected to the cells with Lipofectamine RNAiMAX (Invitrogen) reagent as directed in the manufacturer's protocol and with Opti-MEM medium (Invitrogen). After incubation for 24 hours under 5% CO_2 at 37 °C, the cells were lysed with TRIzol reagents (Invitrogen) and total RNAs were extracted in accordance with the manufacturer's protocol.

In vivo *therapeutic experiments in a mouse model of hypercholesterolemia.* All animal experiments were conducted according to the guidelines of the Animal Care Ethics Committee of the National Cerebral and Cardiovascular Center Research Institute (Osaka, Japan). Male C57BL/6J mice (Japan, SLC, Inc., Hamamatsu, Japan) aged 7 weeks were

used in this study. The mice were maintained on a 12-hour light/12-hour dark cycle and fed *ad libitum*. To induce hypercholesterolemia, wild-type C57BL/6J mice were fed an atherogenic diet, F2HFD1, containing 1.25% cholesterol (Oriental Yeast, Tokyo, Japan) from the beginning one week before administration of any siRNA and throughout the experiment.

To deliver each siRNA, we used Invivofectamine 2.0 reagent (Invitrogen) according to the manufacturer's instructions. Five mg/kg of each siRNA was formulated with Invivofectamine 2.0 reagent, and each mouse received one siRNA (siNTC-trl, siApoB-1, siLNA-2, siL2PT-1, siL2PTC-1, siL2PTC-1M, siL2PTC-1L, siL2PT-1M, and siApoB-1C) as an siRNA–Invivofectamine 2.0 complex via tail vein injection. The physical appearance and body weight of each mouse were recorded during this study. Before an animal was sacrificed, a blood sample was collected from the tail vein using BD Microtainers (BD, Franklin Lakes, NJ). Each of these blood samples was subsequently subjected to centrifugation. TC levels in serum samples were measured using Cholesterol E (Wako, Osaka, Japan) according to the manufacturer's instructions with adjustment for a 96-well microplate. Mice ($N = 3–5$) were sacrificed 2, 7, 14, or 24 days after injection of siRNA. Mice were anesthetized before being sacrificed, and samples of whole blood were collected from each inferior vena cava to measure the activity of AST and ALT and to quantify the BUN and creatinine levels. Next, the liver and kidneys of each animal were harvested to quantify apoB mRNA levels using quantitative PCR; samples of liver tissue and kidney tissue were also collected for histopathological analysis.

Six hours after injection of each siRNA, we collected a blood sample from the tail vein of each mouse. We processed each of these samples to assess serum levels of IFN-α using an IFN-α enzyme-linked immunosorbent assay kit (PBL Interferon Source, Piscataway, NJ) according to the manufacturer's directions.

Harvested liver samples were cut into 2 × 2 mm squares and immediately frozen using liquid nitrogen. For each mouse, one 2 × 2 mm square was put into 1 ml of TRIzol reagent (Invitrogen) for homogenization, and total RNA was isolated in accordance with the manufacturer's protocol accompanying the TRIzol regent.

Quantitative PCR analysis. We used a High-Capacity cDNA Reverse Transcription Kit (Applied Biosystems, Foster City, CA) to prepare cDNA from 10 µg of each sample of total RNA extracted from cells or tissues. Each cDNA sample was subjected to Real-Time PCR (StepOnePlus Real-Time PCR System; Applied Biosystems) to measure the relative quantities of APOB, GAPDH, IFIT-1, and OAS-1 expression using SYBR Green reagent (Applied Biosystems) and of SREBP2, α1 using the TaqMan Gene Expression Assay (Applied Biosystems). The expression levels of target genes were normalized using GAPDH expression as an internal control. The following primer sets were used for quantitative PCR: for mouse ApoB, forward primer 5′-TGGGCAACTT-TACCTATGACTT-3′ and reverse primer 5′-AAGGAAATG-GGCAACGATA-3′; mouse GAPDH, forward primer 5′-CA AAATGGTGAAGGTCGGTGTG-3′ and reverse primer 5′-ATTTGATGTTAGTGGG GTCTCG-3′; mouse IFIT-1, forward primer 5′- AGGCTGGAGTGTGCTGAGAT-3′ and reverse primer 5′- TCTGGATTTAACCGGACAG-3′; mouse OAS1, forward primer 5′-CTGACCTGGTGGTGTTCCTT-3′ and reverse primer 5′-CCACCATGAACTCTGGACCT-3′. TaqMan Gene Expression Assay; assay ID for SREBP2, ACAT-1 CYP7α1 were Mm01306297_g1, Mm00507463_m1 and Mm00484152_m1, respectively. After an amplification consisting of 40 cycles, relative expression of each target was analyzed with SDS analysis software (Applied Biosystems).

ApoB-100 western blot analysis. Mouse liver tissues were homogenized in Ripa Buffer (Sigma-Aldrich, St Louis, MO) containing complete mini (Roche, Indianapolis, IN). Samples were immediately subjected to centrifugation at 4 °C, 13,000*g* for 5 minutes. The supernatant of each sample was collected into an Amicon Ultra centrifugal Filters Ultracel-50k (Millipore, Billerica, MA), and the contents of the supernatant were concentrated by centrifugation at 4 °C, 20,000*g*. The final volume of each retentate was adjusted to 200 µl with PBS, and the total protein concentration of each sample was determined using a BioRad DC protein assay kit (Lowry method; BioRad, Hercules, CA).

Individual samples (50 µg) of total protein in liver homogenates were subjected to electrophoresis on a 3–8% NuPAGE Tris-Acetate Gel (Invitrogen) and transferred to a polyvinylidene-fluoride membrane (Millipore). Membranes were then incubated with Blocking One reagent (Nacalai Tesque, Kyoto, Japan) for 12 hours at 4 °C for block nonspecific antibody binding. Membranes were then incubated with primary antibody for mouse apoB-100 or -48 (Meridian Life Science, Inc., Saco, ME) for 2 hours at room temperature. After incubation with primary antibody, each membrane was washed with PBS-containing 0.1% of Tween 20, and then the membranes were incubated with goat anti-rabbit immunoglobulin G secondary antibody conjugated with peroxidase (Santa Cruz Biotechnology, Santa Cruz, CA) dissolved in PBS containing 0.1% of Tween 20-containing 0.5% blocking one reagent for 2 hours at room temperature. Protein bands were visualized using the ECL Advance Western blot detection kit (Amersham Biosciences, Buckinghamshire, UK) according to the manufacturer's directions. Images of each western blot were taken with a LAS-4000 mini image analyzer (FUJIFILM), and the intensity of each band was measured using Image J software (http://rsbweb.nih.gov/ij/), which is freely available on the Internet.

Hepatotoxicity and nephrotoxicity assay. To assess the hepatotoxicity associated with each siRNA, we measured the activities of AST and ALT using a GOT·GTP CII kit (Wako) according to the manufacturer's protocol adjusted to 96-well microplate. Results from these assays are presented as AST and ALT activity in IU/L units. As the nephrotoxicities, BUN values in the serum of each sample were measured using a Urea Nitrogen B-test Wako (Wako) kit, and creatinine values in the serum of each sample were measured using FUJI DRI-CHEM CRE-P III with a FUJI DRI-CHEM instrument (FUJIFILM). The Urea Nitrogen B-test Wako was used in accordance with the manufacturer's protocol adjusted to 96-well microplate.

Histopathological analysis. Harvested liver and kidney samples were sectioned and processed for histopathological analysis. Liver and kidney specimens were fixed in 10 %

formalin-PBS (formaldehyde was diluted with PBS, formaldehyde; Wako) for 2 days at room temperature and processed through to paraffin embedding. Routinely, we picked upper and lower lobe regions of the liver and picked kidney tissue including the renal pelvis. All paraffin-embedded tissues were sliced into 5-μm-thick sections using a microtome (Leica Microsystems, Wetzlar, Germany). These sections were stained with Carrazzi's hematoxylin and eosin (Sakura Finetek USA, Inc., Torrance, CA) solutions for histopathological examination.

Statistical analysis. Therapeutic experiments *in vivo* were performed such that for each time point (day 2, 7, 14, and 24), there were 3–5 mice in each treatment group. A Student's *t*-test was performed for comparison of two arms. Values of $P < 0.05$ or $P < 0.01$ were considered to indicate statistical significance.

Acknowledgments. We thank E. Shibata, M. Inoue, M. Morimoto, and M. Sone who are all affiliated with the National Cerebral and Cardiovascular Center Research Institute, for their technical support. This work was supported by Grants-in-Aid for Scientific Research from the Japanese Ministry of Health, Labor and Welfare (H20-genomu-008 and H23-seisa-kutansaku-ippan-004) and by the Program for the Promotion of Fundamental Studies in Health Sciences of the National Institute of Biomedical Innovation (NBIO) of Japan.

Supplementary material

Figure S1. Relative serum total cholesterol (TC) levels on day 40 in the siLNA-2 or siL2PT-1 treated group.
Figure S2. Correlation of apoB mRNA recovery and apoB-100 protein recovery.
Figure S3. Stability of siRNAs toward RNase T.
Figure S4. RIG-I mRNA expression in the liver on day 2 in the siL2PT-1-, siL2PTC-1-, siApoB-1- or siApoB-1C-treated groups.
Figure S5. SREBP2 and ACAT-1 mRNA expression in the liver on day 2 in the siApoB-1- or siApoB-1C-treated groups.
Figure S6. CYP7α1 mRNA expression in the liver on day 2.
Materials and Methods.

1. Hannon, GJ (2002). RNA interference. *Nature* **418**: 244–251.
2. McManus, MT and Sharp, PA (2002). Gene silencing in mammals by small interfering RNAs. *Nat Rev Genet* **3**: 737–747.
3. White, PJ (2008). Barriers to successful delivery of short interfering RNA after systemic administration. *Clin Exp Pharmacol Physiol* **35**: 1371–1376.
4. Chiu, YL and Rana, TM (2003). siRNA function in RNAi: a chemical modification analysis. *RNA* **9**: 1034–1048.
5. De Paula, D, Bentley, MV and Mahato, RI (2007). Hydrophobization and bioconjugation for enhanced siRNA delivery and targeting. *RNA* **13**: 431–456.
6. Shim, MS and Kwon, YJ (2010). Efficient and targeted delivery of siRNA in vivo. *FEBS J* **277**: 4814–4827.
7. Davidson, BL and McCray, PB Jr (2011). Current prospects for RNA interference-based therapies. *Nat Rev Genet* **12**: 329–340.
8. Kuwahara, H, Nishina, K, Yoshida, K, Nishina, T, Yamamoto, M, Saito, Y *et al.* (2011). Efficient *in vivo* delivery of siRNA into brain capillary endothelial cells along with endogenous lipoprotein. *Mol Ther* **19**: 2213–2221.
9. Semple, SC, Akinc, A, Chen, J, Sandhu, AP, Mui, BL, Cho, CK *et al.* (2010). Rational design of cationic lipids for siRNA delivery. *Nat Biotechnol* **28**: 172–176.
10. Love, KT, Mahon, KP, Levins, CG, Whitehead, KA, Querbes, W, Dorkin, JR *et al.* (2010). Lipid-like materials for low-dose, *in vivo* gene silencing. *Proc Natl Acad Sci USA* **107**: 1864–1869.
11. Ge, Q, Dallas, A, Ilves, H, Shorenstein, J, Behlke, MA and Johnston, BH (2010). Effects of chemical modification on the potency, serum stability, and immunostimulatory properties of short shRNAs. *RNA* **16**: 118–130.
12. Chernolovskaya, EL and Zenkova, MA (2010). Chemical modification of siRNA. *Curr Opin Mol Ther* **12**: 158–167.
13. Obika, S, Rahman, SMA, Fujisaka, A, Kawada, Y, Baba, T, and Imanishi, T (2010). Bridged nucleic acids: development, synthesis and properties. *Heterocycles* **81**: 1347–1392.
14. Imanishi, T, and Obika, S (2002). BNAs: novel nucleic acid analogus with a bridged sugar moiety. *ChemComm*: **6**.
15. Elmén, J, Thonberg, H, Ljungberg, K, Frieden, M, Westergaard, M, Xu, Y *et al.* (2005). Locked nucleic acid (LNA) mediated improvements in siRNA stability and functionality. *Nucleic Acids Res* **33**: 439–447.
16. Bramsen, JB, Laursen, MB, Damgaard, CK, Lena, SW, Babu, BR, Wengel, J *et al.* (2007). Improved silencing properties using small internally segmented interfering RNAs. *Nucleic Acids Res* **35**: 5886–5897.
17. Bramsen, JB, Pakula, MM, Hansen, TB, Bus, C, Langkjær, N, Odadzic, D *et al.* (2010). A screen of chemical modifications identifies position-specific modification by UNA to most potently reduce siRNA off-target effects. *Nucleic Acids Res* **38**: 5761–5773.
18. Bramsen, JB, Laursen, MB, Nielsen, AF, Hansen, TB, Bus, C, Langkjaer, N *et al.* (2009). A large-scale chemical modification screen identifies design rules to generate siRNAs with high activity, high stability and low toxicity. *Nucleic Acids Res* **37**: 2867–2881.
19. Abdur Rahman, SM, Sato, H, Tsuda, N, Haitani, S, Narukawa, K, Imanishi, T *et al.* (2010). RNA interference with 2′,4′-bridged nucleic acid analogues. *Bioorg Med Chem* **18**: 3474–3480.
20. Jurk, M, Chikh, G, Schulte, B, Kritzler, A, Richardt-Pargmann, D, Lampron, C *et al.* (2011). Immunostimulatory potential of silencing RNAs can be mediated by a non-uridine-rich toll-like receptor 7 motif. *Nucleic Acid Ther* **21**: 201–214.
21. Allerson, CR, Sioufi, N, Jarres, R, Prakash, TP, Naik, N, Berdeja, A *et al.* (2005). Fully 2'-modified oligonucleotide duplexes with improved *in vitro* potency and stability compared to unmodified small interfering RNA. *J Med Chem* **48**: 901–904.
22. Samuel-Abraham, S and Leonard, JN (2010). Staying on message: design principles for controlling nonspecific responses to siRNA. *FEBS J* **277**: 4828–4836.
23. Goldstein, JL (2001). Laskers for 2001: knockout mice and test-tube babies. *Nat Med* **7**: 1079–1080.
24. Durrington, P (2003). Dyslipidaemia. *Lancet* **362**: 717–731.
25. Soutschek, J, Akinc, A, Bramlage, B, Charisse, K, Constien, R, Donoghue, M *et al.* (2004). Therapeutic silencing of an endogenous gene by systemic administration of modified siRNAs. *Nature* **432**: 173–178.
26. Khvorova, A, Reynolds, A and Jayasena, SD (2003). Functional siRNAs and miRNAs exhibit strand bias. *Cell* **115**: 209–216.
27. Schwarz, DS, Hutvágner, G, Du, T, Xu, Z, Aronin, N and Zamore, PD (2003). Asymmetry in the assembly of the RNAi enzyme complex. *Cell* **115**: 199–208.
28. Kennedy, S, Wang, D and Ruvkun, G (2004). A conserved siRNA-degrading RNase negatively regulates RNA interference in C. elegans. *Nature* **427**: 645–649.
29. Volkov, AA, Kruglova, NS, Meschaninova, MI, Venyaminova, AG, Zenkova, MA, Vlassov, VV *et al.* (2009). Selective protection of nuclease-sensitive sites in siRNA prolongs silencing effect. *Oligonucleotides* **19**: 191–202.
30. Mook, OR, Baas, F, de Wissel, MB and Fluiter, K (2007). Evaluation of locked nucleic acid-modified small interfering RNA *in vitro* and in vivo. *Mol Cancer Ther* **6**: 833–843.
31. Liu, L, Botos, I, Wang, Y, Leonard, JN, Shiloach, J, Segal, DM *et al.* (2008). Structural basis of toll-like receptor 3 signaling with double-stranded RNA. *Science* **320**: 379–381.
32. Judge, AD, Bola, G, Lee, AC and MacLachlan, I (2006). Design of noninflammatory synthetic siRNA mediating potent gene silencing in vivo. *Mol Ther* **13**: 494–505.
33. Hornung, V, Guenthner-Biller, M, Bourquin, C, Ablasser, A, Schlee, M, Uematsu, S *et al.* (2005). Sequence-specific potent induction of IFN-α by short interfering RNA in plasmacytoid dendritic cells through TLR7. *Nat Med* **11**: 263–270.
34. McCarroll, J, Baigude, H, Yang, CS and Rana, TM (2010). Nanotubes functionalized with lipids and natural amino acid dendrimers: a new strategy to create nanomaterials for delivering systemic RNAi. *Bioconjug Chem* **21**: 56–63.
35. Aronin, N (2006). Target selectivity in mRNA silencing. *Gene Ther* **13**: 509–516.
36. Jackson, AL, Burchard, J, Leake, D, Reynolds, A, Schelter, J, Guo, J *et al.* (2006). Position-specific chemical modification of siRNAs reduces "off-target" transcript silencing. *RNA* **12**: 1197–1205.
37. Carthew, RW and Sontheimer, EJ (2009). Origins and Mechanisms of miRNAs and siRNAs. *Cell* **136**: 642–655.
38. Matranga, C, Tomari, Y, Shin, C, Bartel, DP and Zamore, PD (2005). Passenger-strand cleavage facilitates assembly of siRNA into Ago2-containing RNAi enzyme complexes. *Cell* **123**: 607–620.
39. Leuschner, PJ, Ameres, SL, Kueng, S and Martinez, J (2006). Cleavage of the siRNA passenger strand during RISC assembly in human cells. *EMBO Rep* **7**: 314–320.
40. Rossi, JJ (2009). Cholesterol paves the way for topically applied viricides. *Cell Host Microbe* **5**: 6–7.
41. Ambardekar, VV, Han, HY, Varney, ML, Vinogradov, SV, Singh, RK and Vetro, JA (2011). The modification of siRNA with 3' cholesterol to increase nuclease protection and suppression of native mRNA by select siRNA polyplexes. *Biomaterials* **32**: 1404–1411.

42. Haley, B and Zamore, PD (2004). Kinetic analysis of the RNAi enzyme complex. *Nat Struct Mol Biol* **11**: 599–606.
43. Marques, JT, Devosse, T, Wang, D, Zamanian-Daryoush, M, Serbinowski, P, Hartmann, R *et al.* (2006). A structural basis for discriminating between self and nonself double-stranded RNAs in mammalian cells. *Nat Biotechnol* **24**: 559–565.
44. Kato, H, Takeuchi, O, Mikamo-Satoh, E, Hirai, R, Kawai, T, Matsushita, K *et al.* (2008). Length-dependent recognition of double-stranded ribonucleic acids by retinoic acid-inducible gene-I and melanoma differentiation-associated gene 5. *J Exp Med* **205**: 1601–1610.
45. Gao, S, Dagnaes-Hansen, F, Nielsen, EJ, Wengel, J, Besenbacher, F, Howard, KA *et al.* (2009). The effect of chemical modification and nanoparticle formulation on stability and biodistribution of siRNA in mice. *Mol Ther* **17**: 1225–1233.
46. Caffrey, DR, Zhao, J, Song, Z, Schaffer, ME, Haney, SA, Subramanian, RR *et al.* (2011). siRNA off-target effects can be reduced at concentrations that match their individual potency. *PLoS ONE* **6**: e21503.

Supplementary Information accompanies this paper on the Molecular Therapy–Nucleic Acids website (http://www.nature.com/mtna)

Organic & Biomolecular Chemistry

Cite this: *Org. Biomol. Chem.*, 2012, **10**, 5102

www.rsc.org/obc

PAPER

Synthesis and evaluation of novel caged DNA alkylating agents bearing 3,4-epoxypiperidine structure†

Yuji Kawada,‡[a] Tetsuya Kodama,‡[a] Kazuyuki Miyashita,[b] Takeshi Imanishi[a] and Satoshi Obika*[a]

Received 21st February 2012, Accepted 30th April 2012
DOI: 10.1039/c2ob25366f

Previously, we reported that the 3,4-epoxypiperidine structure, whose design was based on the active site of DNA alkylating antitumor antibiotics, azinomycins A and B, possesses prominent DNA cleavage activity. In this report, novel caged DNA alkylating agents, which were designed to be activated by UV irradiation, were synthesized by the introduction of four photo-labile protecting groups to a 3,4-epoxypiperidine derivative. The DNA cleavage activity and cytotoxicity of the caged DNA alkylating agents were examined under UV irradiation. Four caged DNA alkylating agents showed various degrees of bioactivity depending on the photosensitivity of the protecting groups.

Introduction

The first documented use of a cancer therapeutic agent was a DNA alkylating agent, nitrogen mustard, in 1958.[1] This report showed that nitrogen mustard, which was created as a chemical weapon during World War II, exhibited drug potency for neoplastic disease. Starting with this first application of a cancer therapy, more efficient and harmless DNA alkylating agents have been created and used as means to treat cancer.[2,3] Even now, more efficient DNA alkylating agents with fewer side effects are desired.

Biologically active substances that are modified by a photo-labile protecting group to make them temporarily inactive and that can express their original bioactivity by photo irradiation are called "caged compounds".[4] Expression of the activity is confined to the time and position of irradiation. This behavior enables caged compounds to accomplish spatiotemporal control of bioactivity. Caging of DNA alkylating agents is anticipated to allow site-specific anticancer activity upon light irradiation and, accordingly, avoidance of systemic side effects such as myelosuppression. Many photo-inducible DNA damaging or cytotoxic compounds have been reported in the past.[5–11] However, to our knowledge, there are few reported cases of photo-triggered DNA alkylating agents.[12,13] Herein, we report novel caged DNA alkylating agents. We introduced four typical photo-labile protecting groups into a DNA alkylating agent 3,4-epoxypiperidine derivative, and examined DNA cleavage activity and cytotoxicity under UV irradiation.

[a]*Graduate School of Pharmaceutical Sciences, Osaka University, 1-6 Yamadaoka, Suita, Osaka 565-0871, Japan. E-mail: obika@phs.osaka-u.ac.jp; Fax: +81 6 6879 8204; Tel: +81 6 6879 8200*
[b]*Faculty of Pharmacy, Osaka Ohtani University, 3-11-1 Nishikiorikita, Tondabayashi, Osaka 584-8540, Japan*

† Electronic supplementary information (ESI) available: NMR-spectra of new compounds, and UV-absorption spectra and result of agarose gel shift assay of **3** and **4a–4d** in the presence of radical scavenger. See DOI: 10.1039/c2ob25366f

‡ These authors contributed equally to this study.

Results and discussion

Design and synthesis of caged DNA alkylating agents

Previously, we have hypothesized that the 4-hydroxy-1-azabicyclo-[3.1.0]hexane structure which is the active site of DNA alkylating natural products, azinomycins A and B, and the 3,4-epoxypiperidine structure could interconvert.[14] And indeed, we found that 3,4-epoxypiperidine derivatives possess potent DNA cleavage activity.[14] It is also found out that the secondary amine structure in the piperidine motif was important for the DNA cleavage activity, and therefore a modification at the piperidinic nitrogen atom of 3,4-epoxypiperidine derivatives caused less activity.[14] 3,4-Epoxypiperidine **3** bearing a phenyl triazolyl group, which was recently synthesized as a part of our 3,4-epoxypiperidine library,[15] has both the potent DNA cleavage activity and the chemical stability under isolated conditions, while most other 3,4-epoxypiperidine derivatives in the library are relatively unstable at concentrated solution conditions. These unique properties of 3,4-epoxypiperidine **3** encouraged us to prepare the corresponding caged DNA alkylating agents by a modification of the piperidinic secondary amine with photo-labile protecting group.

Four common protecting groups, *o*-nitrobenzyloxycarbonyl group (**a**),[16] 3,5-dimethoxybenzyloxycarbonyl group (**b**),[17] 3,4-dimethoxy-6-nitrobenzyloxycarbonyl group (**c**)[18,19] and α-methyl-*o*-nitrobenzyloxycarbonyl group (**d**),[20] were selected as photo-labile protecting groups. *o*-Nitrobenzyloxycarbonyl- (**a**), 3,4-dimethoxy-6-nitrobenzyloxycarbonyl- (**c**), and α-methyl-*o*-

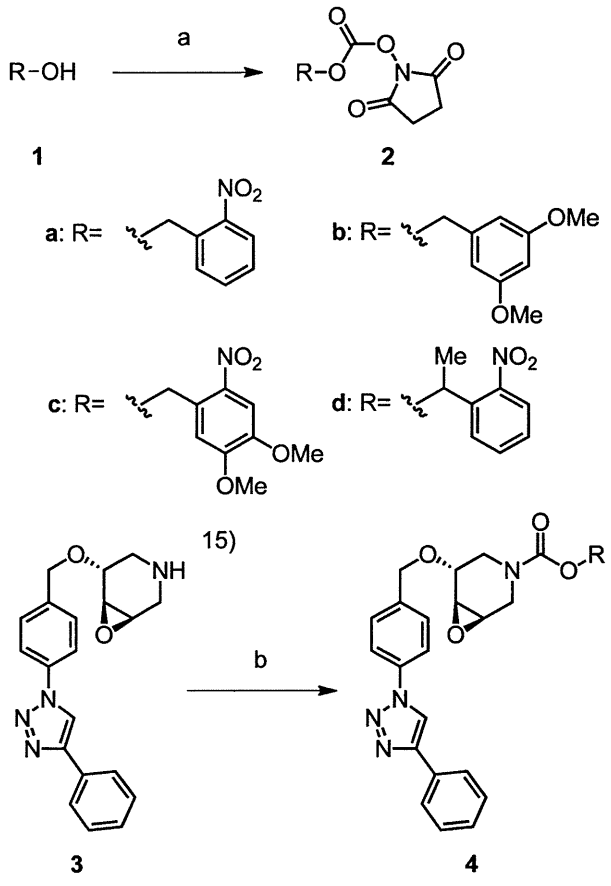

Scheme 1 Reagents and conditions: (a) disuccinimidyl carbonate, triethylamine, MeCN, 66%–quant.; (b) **2**, triethylamine, CH_2Cl_2, 74–97%.

nitrobenzyloxycarbonyl group (**d**) would be sensitive to a relatively harmless 365 nm of wavelength, whereas 3,5-dimethoxybenzyloxycarbonyl group (**b**) which requires much shorter 254 nm of wavelength for the activation should be insensitive as long as 365 nm of wavelength is irradiated.[21]

First, active carbonates **2a–2d** were synthesized from the corresponding alcohols **1a–1d** by treatment with disuccinimidyl carbonate. Conversion of 3,4-epoxypiperidine **3** to caged DNA alkylating agents **4a–d** was accomplished by the treatment of **3** with the carbonates **2a–2d** (Scheme 1).

DNA relaxation assay

We examined by a relaxation assay of supercoiled plasmid DNA pBR 322 whether the caged DNA alkylating agents **4a–4d** could restore the native activity of **3** by UV irradiation. After the addition of each of the caged alkylating agents to a solution of plasmid DNA, UV irradiation (365 nm) was applied for the indicated period of time, and then incubated for 24 h at 37 °C. The alteration of plasmid DNA was analyzed by agarose gel electrophoresis (Fig. 1). As shown in Fig. 1a, activation of **4a–4d** by UV irradiation resulted in the transformation of the supercoiled plasmid DNA (form I) into an open circular DNA (form II). Fig. 1b–1f summarize the relationship between the UV irradiation period and DNA cleavage activity. The DNA cleavage activity is represented by the ratio of form I to form II of plasmid DNA. Without UV irradiation, all of the caged DNA alkylating agents **4a–4d** were inactive while the original 3,4-epoxypiperidine **3** converted form I to form II of plasmid. When UV irradiation was applied for 2 s, with 10 μM of caged alkylating agent, compound **4d** was activated, resulting in cleavage of approximately 50% of plasmid DNA, and **4a** and **4c** showed some activity. On the other hand, compound **4b** was not active toward plasmid DNA. After 5 s of irradiation, compound **4d** was activated completely, showing DNA cleavage activity equivalent to positive control **3**. In 5 s, compounds **4a** and **4c** expressed stronger DNA cleavage activity than under a 2 s irradiation period. Compound **4b** again showed no activity. When the irradiation period was prolonged to 15 or 60 s, compound **4b** was still inactive. The activity of **4a** grew depending on the irradiation period. In contrast, the activity of **4c** plateaued at about 50% even for an irradiation period of 60 s.

As observed above, the four caged DNA alkylating agents **4a–4d** showed different behavior toward UV irradiation. Most of this result can be explained as the differing photo-sensitivity of each four protecting groups. First of all, **4b** was inactive as we designed. A result that the activation of **4d** was much faster than that of **4a** and **4c** was consisted with a report by Hasan *et al.*[22] They described that mono-substitution at the α-position of the nitrobenzyl group makes abstraction of the benzylic hydrogen atom easier, consequently accelerating the photo-induced deprotection.[22]

The progress of the uncaging reaction is generally dependent on the irradiation period. The activation of **4a** and **4d** also irradiation-period-dependently proceeded and respectively completed within 1 min and 5 s. But in the case of **4c**, form-conversion of plasmid reached the plateau in mid course. Because the activity of **3** itself did not change whether nitrosobenzaldehyde co-existed or not (data not shown), it is considered that this phenomenon resulted from generation of 3,4-dimethoxy-6-nitrosobenzaldehyde from compound **4c** which potently absorbed UV rays, and conversion of **4c** into **3** was interrupted when the concentration of 3,4-dimethoxy-6-nitrosobenzaldehyde reached a certain degree.

Although we suppose that the 3,4-epoxypiperidine derivatives induced DNA cleavage *via* DNA alkylation, the mechanism is not confirmed yet. To exclude the other possibility of DNA cleavage pathway: radical-mediated DNA cleavage[10] induced by a photo irradiation, a plasmid DNA relaxation assay in the presence of hydroxyl radical scavenger (glycerol) or singlet oxygen scavenger (NaN_3) was carried out[10] (ESI, Fig. S1†). As a result, almost no change of DNA cleavage activity was observed despite the presence of scavenger. This result shows that the DNA cleavage activity of epoxypiperidine derivatives **3** and **4a–4d** is not derived from a radical pathway, and supports our assumption that epoxypiperidine derivatives work as DNA alkylating agents.

Cytotoxicity of caged DNA alkylating agents triggered by UV irradiation

The cytotoxicity of caged DNA alkylating agents against HepG2 cells was examined by MTT assay following UV irradiation for 5 s and incubation for 24 h at 37 °C (Fig. 2a and 3). All caged

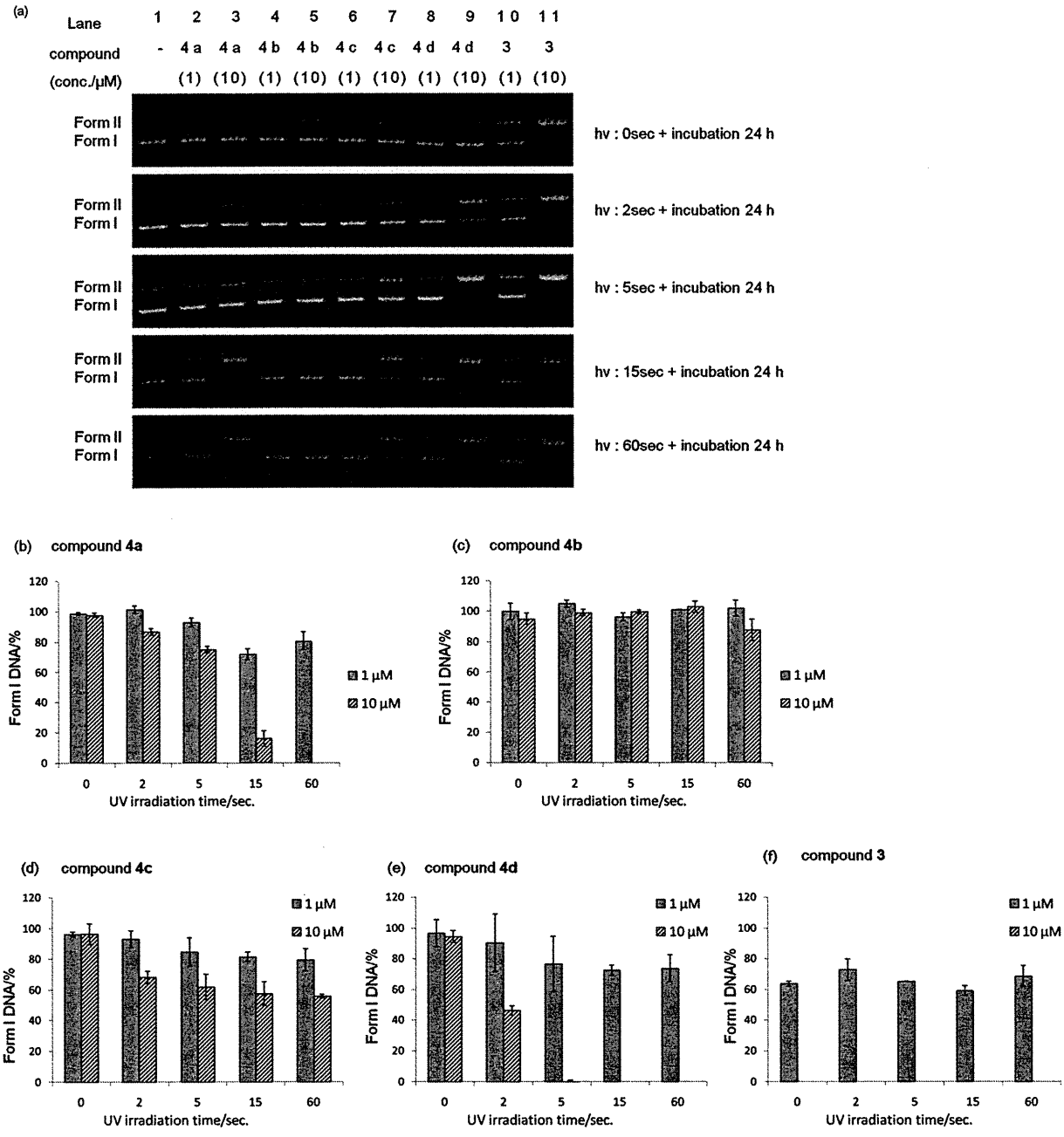

Fig. 1 Plasmid relaxation assay with caged DNA alkylating agents **4a–4d** and **3**. (a) Results of agarose gel shift assay. (b)–(f) Relationship between percentage of intact DNA and UV irradiation time. These are represented as the average of two times.

DNA alkylating agents **4a–4d** were atoxic without UV irradiation. Prominent enhancement of cytotoxicity of **4c** and **4d** at 100 μM were induced by UV irradiation, whereas that of **4a** and **4b** was not affected at all. Compounds **4c** and **4d** showed potent cytotoxicity equal to the parent compound **3** under irradiation conditions. Compound **3** itself did not show any change in activity by UV irradiation. This tendency was in complete agreement with that of the DNA relaxation assay, and indicated that **4c** and **4d** are excellent caged DNA alkylating agents which can express cytotoxicity triggered by UV irradiation.

In regard to this result, we were concerned about the possibility that nitrosobenzene derivatives produced from deprotection of photo-labile protective groups might affect cytotoxicity. Therefore, we synthesized compounds **5a** and **5b** as control compounds (Fig. 4a). These compounds release each nitrosobenzene derivative and noncytotoxic piperidine upon photo-irradiation. The control experiment was achieved in a similar manner to the cytotoxicity assay of **4a–4d**. Compounds **5a** and **5b** showed no cytotoxicity (Fig. 4), *i.e.*, nitrosobenzene derivatives had no potential toward cytotoxicity in our experimental system.

Additionally, caged DNA alkylating agent **4d** possessed an interesting property that its cytotoxicity varied depending on the interval periods between addition of **4d** and UV irradiation. This experiment was conducted as described in Fig. 2b. After 24 h of

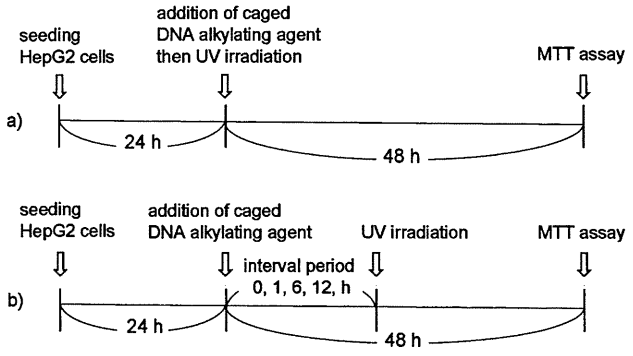

Fig. 2 Diagram of examination of cytotoxicity.

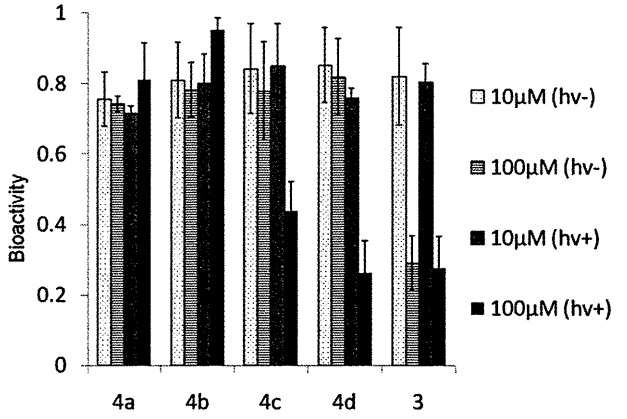

Fig. 3 MTT assay using caged DNA alkylating agents **4a–4d** and non-caged DNA alkylating agent **3** by treatment of UV irradiation for 5 s. The bioactivity is represented as a ratio to control.

HepG2 cells being seeded onto a 96-well plate, compound **4d** was added to each well, and the cells were further incubated for 48 h. UV irradiation was applied at 0, 1, 6 or 12 h (interval period) after addition of **4d**. The living cells were counted by MTT assay (Fig. 5). The cytotoxicity of **4d** was increased as the interval period was extended up to 12 h. In particular, the improvement of the activity was most remarkable at a concentration of 10 μM, and the increase in cytotoxicity was obviously relative to the interval period.

We believe that this behavior can be explained by membrane permeability because parent compound **3** had no cytotoxicity at 10 μM (Fig. 3); on the other hand, compound **4d**, whose amino group was covered by a relatively non-polar α-methyl-*o*-nitrobenzyloxycarbonyl group, showed potent cytotoxicity at the same concentration after an adequate interval and the following photo-irradiation (Fig. 5). It is known that several biologically active agents containing amino groups are less membrane-permeable due to their high polarity, and low membrane permeability provides a disadvantage in drug kinetics. To resolve this problem, conversion into prodrugs by modification on the polar amino group has been reported.[23–26] As in these cases, it is thought that improvement of bioactivity could be derived from altering the membrane permeability by introduction of a photo-labile protecting group.

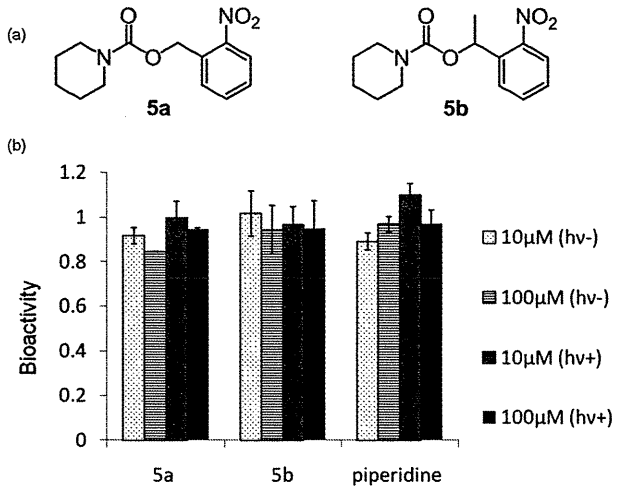

Fig. 4 (a) Structures of control compounds **5a** and **5b**. (b) MTT assay using control compounds **5a**, **5b** and piperidine by treatment of UV irradiation for 5 s. The cytotoxicity is represented as a ratio to control.

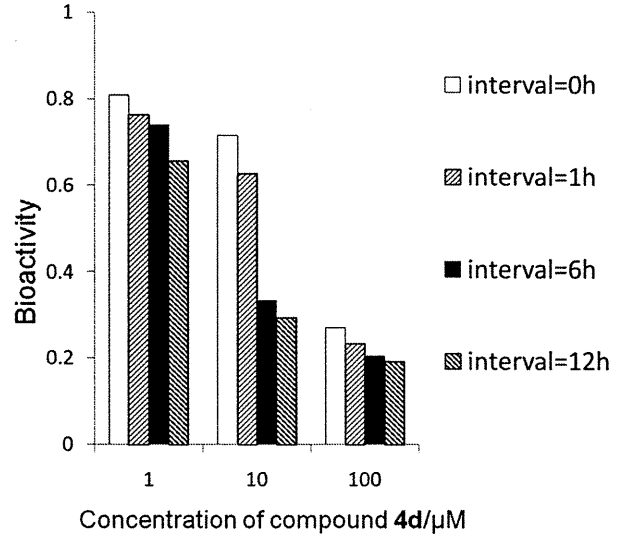

Fig. 5 The dependence between interval period from addition of caged DNA alkylating agent **4d** to UV irradiation and cytotoxicity. The cytotoxicity is represented as a ratio to control.

Conclusion

In this paper, we described the synthesis and biological characteristics of novel caged DNA alkylating agents. The synthesis of compounds **4a–4d** was easily accomplished from 3,4-epoxypiperidine **3** by introduction of four types of photo-labile protecting groups. The results of the DNA relaxation assay indicated that **4c** and **4d** were successfully activated by UV irradiation within 5 s while **4b** scarcely showed DNA cleavage activity at the longest irradiation time (60 s). This tendency closely correlated with the result of the MTT assay. Additionally, cytotoxicity of **4d** varied depending on the timing of UV irradiation. It is considered that this result could be derived from the alteration of polarity by protection of the nitrogen atom, *i.e.*, the caging of epoxypiperidine **3** not only imparts a trigger function by UV

rays but also improves membrane permeability. These results suggested the utility of **4d** as a novel anticancer drug whose activity can be controlled spatiotemporally.

Experimental

General

Unless otherwise noted, all chemicals from commercial sources were used without further purification. CH_2Cl_2 and triethylamine were distilled over calcium hydride. All reactions were carried out under a nitrogen atmosphere. Melting points were measured on a Yanagimoto micro-melting point apparatus and are uncorrected. The ^1H and ^{13}C NMR spectra were recorded on JEOL AL-300 (^1H, 300 MHz; ^{13}C, 75.5 MHz) or JEOL ECS-400 (^1H, 400 MHz; ^{13}C, 100 MHz) instruments. Values of δ are in ppm relative to tetramethylsilane (0.00 ppm) or $CDCl_3$ (7.26 ppm) as internal standards. The IR spectra were recorded on a JASCO FT/IR-4200 spectrometer. FAB-mass or EI-mass were measured on a JEOL JMS-600 or JMS-700 mass spectrometer. Column chromatography was achieved using Fuji Silysia FL-100D or PSQ-100B silica gel. Photoirradiation at 365 nm was performed with a ZUV-C30H UV-LED lamp as a light source and ZUVL8H as a lens unit (Omron, Kyoto, Japan).

2-Nitrobenzyl-*N*-succinimidyl carbonate (2a)

To a solution of 2-nitrobenzyl alcohol (**1a**) (1.0 g, 6.5 mmol) and triethylamine (990 mg, 1.4 mL, 9.8 mmol) in acetonitrile (50 mL) was added disuccinimidyl carbonate (1.8 g, 7.2 mmol), and the reaction mixture was stirred at room temperature for 30 min. The reaction mixture was diluted with AcOEt. The organic layer was washed by water and brine, dried over Na_2SO_4, and concentrated under reduced pressure. The resulting residue was purified by recrystallization (*n*-hexane–toluene = 4 : 1) to give **2a** (1.5 g, 73%) as colorless crystals: mp 120–123 °C; IR ν_{max}/cm^{-1} (KBr) 1812, 1788, 1741, 1526, 1360, 1258, 1235, 1201, 1076, 1058, 1047 cm^{-1}; ^1H NMR ($CDCl_3$, 300 MHz) δ 2.84 (4H, s), 5.78 (2H, s), 7.52–7.57 (1H, m), 7.67–7.56 (2H, m), 8.19 (1H, d, J = 8.0 Hz); ^{13}C NMR ($CDCl_3$, 75 MHz) δ 25.44, 68.67, 125.35, 128.17, 129.38, 130.19, 134.43, 146.78, 151.33, 168.44; Mass (FAB) *m/z* 295 (M + H^+); HRMS (FAB) calcd for $C_{12}H_{11}N_2O_7$: 295.0566. Found: 295.0566.

3,5-Dimethoxybenzyl-*N*-succinimidyl carbonate (2b)

To a solution of 3,5-dimethoxybenzyl alcohol (**1b**) (500 mg, 3.0 mmol) and triethylamine (450 mg, 0.63 mL, 4.5 mmol) in acetonitrile (20 mL) was added disuccinimidyl carbonate (840 mg, 3.3 mmol), and the reaction mixture was stirred at room temperature for 20 min. The reaction mixture was diluted with CH_2Cl_2. The organic layer was washed by water and brine, dried over Na_2SO_4, and concentrated under reduced pressure. The resulting residue was purified by recrystallization (*n*-hexane–toluene = 4 : 1) to give **2b** (0.92 g, quant.) as colorless crystals: mp 78–80 °C; IR ν_{max}/cm^{-1} (KBr) 1813, 1789, 1742, 1600, 1465, 1432, 1377, 1325, 1208, 1091, 1069; ^1H NMR (300 MHz; $CDCl_3$) δ 2.84 (4H, s), 3.80 (6H, s), 5.25 (2H, s), 6.46 (1H, d, J = 1.5 Hz), 6.52 (1H, d, J = 1.5 Hz); ^{13}C NMR (75 MHz; $CDCl_3$) δ 25.42, 55.41, 72.59, 101.24, 105.96, 135.35, 151.56, 161.02, 168.55; Mass (FAB) *m/z* 332 (M + Na^+); HRMS (FAB) calcd for $C_{14}H_{15}N_1O_7Na$: 332.0746. Found: 332.0742.

4,5-Dimethoxy-2-nitrobenzyl-*N*-succinimidyl carbonate (2c)

To a solution of 4,5-dimethoxy-2-nitrobenzyl alcohol (**1c**) (500 mg, 2.4 mmol) and triethylamine (360 mg, 0.49 mL, 3.5 mmol) in acetonitrile (20 mL) was added disuccinimidyl carbonate (660 mg, 2.6 mmol), and the reaction mixture was stirred at room temperature for 20 min. The reaction mixture was diluted with CH_2Cl_2. The organic layer was washed by water and brine, dried over Na_2SO_4, and concentrated under reduced pressure. The resulting mixture was purified by silica gel column chromatography (AcOEt–*n*-hexane = 1 : 2) to give **2c** (550 mg, 66%) as a pale yellow solid: mp 131–133 °C; IR ν_{max}/cm^{-1} (KBr) 1815, 1789, 1741, 1582, 1525, 1332, 1282, 1217, 1067; ^1H NMR (300 MHz; $CDCl_3$) δ 2.87 (4H, s), 3.98 (s, 3H), 4.07 (3H, s), 5.80 (2H, s), 7.06 (1H, s), 7.77 (1H, s); ^{13}C NMR (75 MHz; $CDCl_3$) δ 25.42, 56.43, 56.65, 69.14, 108.20, 108.60, 125.36, 139.07, 148.49, 151.36, 154.14, 168.44; Mass (FAB) *m/z* 377 (M + Na^+); HRMS (FAB) calcd for $C_{14}H_{14}N_2O_9Na$: 377.0597. Found: 377.0573.

1-(2-Nitrophenyl)ethyl-*N*-succinimidyl carbonate (2d)

To a solution of 2-nitroacetophenone (1.0 g, 6.1 mmol) in ethanol (30 mL) was added $NaBH_4$ (340 mg, 9.1 mmol) at 0 °C, and stirred at rt for 2 h. After addition of water, the resulting mixture was extracted twice with AcOEt. The combined organic layers were washed with water and brine. The organic layer was dried over Na_2SO_4 and concentrated to give 1-(2-nitrophenyl) ethanol (**1d**) as a crude compound. To the crude **1d** was added acetonitrile (30 mL), triethylamine (920 mg, 1.3 mL, 9.1 mmol), and disuccinimidyl carbonate (1.7 g, 6.7 mmol). The reaction mixture was stirred at room temperature for 1 h. The reaction mixture was diluted with CH_2Cl_2. The organic layer was washed by water and brine, dried over Na_2SO_4, and concentrated under reduced pressure. The resulting residue was purified by recrystallization (*n*-hexane–toluene = 6 : 1) to give **2d** (1.6 g, 88%) as colorless crystals: mp 100–101 °C; IR ν_{max}/cm^{-1} (KBr) 1816, 1791, 1741, 1530, 1346, 1259, 1224, 1093; ^1H NMR (300 MHz; $CDCl_3$) δ 1.79 (3H, d, J = 6.5 Hz), 2.79 (4H, s), 6.39 (1H, q, J = 6.5 Hz), 7.51 (1H, ddd, J = 2.5, 7.0, 7.0 Hz), 7.71–7.75 (2H, m), 8.02 (1H, d, J = 8.0 Hz); ^{13}C NMR (75 MHz; $CDCl_3$) δ 22.07, 25.34, 75.92, 124.70, 126.90, 129.18, 134.27, 135.78, 147.14, 150.64, 168.43; Mass (FAB) *m/z* 309 (M + H^+); HRMS (FAB) calcd for $C_{13}H_{13}N_2O_7$: 309.0723. Found: 309.0714.

(3*RS*,4*RS*,5*RS*)-3,4-Epoxy-*N*-(2-nitrobenzyloxycarbonyl)-5-[4-(4-phenyl-1*H*-1,2,3-triazol-1-yl)benzyloxy]piperidine (4a)

To a solution of **3** (100 mg, 0.29 mmol) and triethylamine (44 mg, 60 μL, 0.44 mmol) in CH_2Cl_2 (3.0 mL) was added **2a**

(93 mg, 0.32 mmol), and the reaction mixture was stirred at room temperature for 1 h. The reaction mixture was diluted with AcOEt. The organic layer was washed by water and brine, dried over Na_2SO_4, and concentrated under reduced pressure. The resulting residue was purified by silica gel column chromatography (AcOEt–*n*-hexane = 1 : 1) to give **4a** (138 mg, 91%) as a white solid: mp 132–133 °C; IR ν_{max}/cm^{-1} (KBr) 1703, 1523, 1461, 1427, 1341, 1233, 1125, 1097; ^1H NMR (400 MHz; $CDCl_3$) δ 3.32–3.35 (2H, m), 3.47 (1H, ddd, J = 3.0, 14.5, 18.0 Hz), 3.65 (1H, ddd, J = 5.0, 14.0 Hz), 3.85–3.98 (3H, m), 4.62–4.82 (2H, m), 5.50–5.57 (2H, m), 7.36–7.63 (8H, m), 7.77 (2H, dd, J = 4.5, 8.0 Hz), 7.92 (1H, d, J = 8.0 Hz), 8.08 (1H, d, J = 8.0 Hz), 8.19 (1H, s); ^{13}C NMR (75 MHz; DMSO-d_6, 80 °C) δ 41.54, 41.65, 49.35, 51.15, 62.81, 69.66, 69.90, 119.04, 119.64, 124.07, 125.10, 127.72, 128.44, 128.65, 128.78, 130.04, 131.48, 133.31, 135.72, 138.44, 147.02, 147.27, 154.20; Mass (FAB) *m/z* 528 (M + H^+); HRMS (FAB) calcd for $C_{28}H_{26}N_5O_6$: 528.1883. Found: 528.1895; *Anal.* Calcd for $C_{28}H_{25}N_5O_6$: C, 63.75; H, 4.78; N, 13.28. Found: C, 63.81; H, 4.86; N, 13.22.

(3*RS*,4*RS*,5*RS*)-*N*-(3,5-Dimethoxybenzyloxycarbonyl-3,4-epoxy)-5-[4-(4-phenyl-1*H*-1,2,3-triazol-1-yl)benzyloxy]piperidine (4b)

To a solution of **3** (50 mg, 0.14 mmol) and triethylamine (22 mg, 30 μL, 0.22 mmol) in CH_2Cl_2 (1.5 mL) was added **2b** (49 mg, 0.16 mmol), and the reaction mixture was stirred at room temperature for 30 min. The reaction mixture was diluted with AcOEt. The organic layer was washed by water and brine, dried over Na_2SO_4, and concentrated under reduced pressure. The resulting mixture was purified by silica gel column chromatography (AcOEt–*n*-hexane = 1 : 1) to give **4b** (58 mg, 74%) as a white solid: mp 73–77 °C; IR ν_{max}/cm^{-1} (KBr) 1698, 1598, 1521, 1459, 1424, 1360, 1322, 1281, 1234, 1205, 1154, 1125, 1092, 1070, 1038; ^1H NMR (400 MHz; $CDCl_3$) δ 3.28–3.33 (2H, m), 3.46 (1H, dd, J = 3.0, 14.0 Hz), 3.63 (1H, dd, J = 5.0, 14.0 Hz), 3.75 (3H, s), 3.78 (3H, s), 3.85–3.98 (3H, m), 4.61–4.85 (2H, m), 5.05–5.01 (2H, m), 6.41 (1H, s), 6.50 (2H, s), 7.36–7.54 (5H, m), 7.72 (1H, d, J = 8.0 Hz), 7.77 (1H, d, J = 8.0 Hz), 7.92 (2H, d, J = 8.0 Hz), 8.20 (1H, s); ^{13}C NMR (75 MHz; DMSO-d_6, 80 °C) δ 41.54, 41.60, 49.38, 51.21, 54.83, 65.88, 69.65, 69.93, 99.40, 105.08, 119.04, 119.65, 125.10, 127.72, 128.45, 130.05, 135.72, 138.45, 138.81, 147.03, 154.65, 160.31; Mass (FAB) *m/z* 543 (M + H^+); HRMS (FAB) calcd for $C_{30}H_{31}N_4O_6$: 543.2244. Found: 543.2225.

(3*RS*,4*RS*,5*RS*)-*N*-(4,5-Dimethoxy-2-nitrobenzyloxycarbonyl)-3,4-epoxy-5-[4-(4-phenyl-1*H*-1,2,3-triazol-1-yl)benzyloxy]-piperidine (4c)

To a solution of **3** (50 mg, 0.14 mmol) and triethylamine (22 mg, 30 μL, 0.22 mmol) in CH_2Cl_2 (1.5 mL) was added **2c** (56 mg, 0.16 mmol), and the reaction mixture was stirred at room temperature for 30 min. The reaction mixture was diluted with AcOEt. The organic layer was washed by water and brine, dried over Na_2SO_4, and concentrated under reduced pressure. The resulting mixture was purified by silica gel column chromatography (AcOEt–*n*-hexane = 1 : 1) to give **4c** (62 mg, 74%) as a pale yellow foam: IR ν_{max}/cm^{-1} (KBr) 1704, 1580, 1522, 1459, 1433, 1362, 1328, 1278, 1247, 1220, 1123, 1093, 1067, 1037; ^1H NMR (400 MHz; $CDCl_3$) δ 3.30–3.33 (2H, m), 3.57 (1H, dd, J = 5.0, 13.0 Hz), 3.59 (1H, d, J = 5.0 Hz), 3.91 (6H, s), 3.92–4.07 (3H, m), 4.62–4.81 (2H, m), 5.42–5.64 (2H, m), 6.94 (1H, s), 7.37–7.40 (1H, m), 7.42–7.51 (4H, m), 7.71–7.76 (3H, m), 7.93 (2H, d, J = 8.0 Hz), 8.22 (1H, s); ^{13}C NMR (75 MHz; DMSO-d_6, 90 °C) δ 41.59, 41.74, 49.32, 51.23, 55.87, 55.91, 62.99, 69.66, 69.85, 99.65, 108.41, 111.02, 118.91, 119.55, 125.07, 126.50, 127.65, 128.37, 130.02, 135.70, 138.36, 139.54, 146.98, 147.81, 153.07, 154.27; Mass (FAB) *m/z* 588 (M + H^+); HRMS (FAB) calcd for $C_{30}H_{30}N_5O_8$: 588.2094. Found: 588.2097.

(3*RS*,4*RS*,5*RS*)-3,4-Epoxy-*N*-(1-(2-nitrophenyl)ethoxycarbonyl)-5-[4-(4-phenyl-1*H*-1,2,3-triazol-1-yl)benzyloxy]piperidine (4d)

To a solution of **3** (100 mg, 0.29 mmol) and triethylamine (44 mg, 60 μL, 0.44 mmol) in CH_2Cl_2 (3.0 mL) was added **2d** (88 mg, 0.29 mmol), and the reaction mixture was stirred at room temperature for 10 min. The reaction mixture was diluted with AcOEt. The organic layer was washed by water and brine, dried over Na_2SO_4, and concentrated under reduced pressure. The resulting mixture was purified by silica gel column chromatography (AcOEt–*n*-hexane = 1 : 1) to give a diastereomixture of **4d** (150 mg, 97%) as a white foam: IR ν_{max}/cm^{-1} (KBr) 1698, 1523, 1458, 1425, 1354, 1248, 1125, 1091, 1039; ^1H NMR (400 MHz; $CDCl_3$) δ 1.65–1.67 (3H, m), 3.32–3.87 (4H, m), 3.96–3.98 (2H, m), 4.52–4.89 (2H, m), 6.19–6.29 (1H, s), 7.33–7.92 (10H, m), 7.86–7.96 (3H, m), 8.17–8.22 (1H, m); Mass (FAB) *m/z* 542 (M + H^+); HRMS (FAB) calcd for $C_{29}H_{28}N_5O_6$: 542.2040. Found: 542.2047.

***N*-2-Nitrobenzyloxycarbonylpiperidine (5a)**

To a solution of piperidine (100 mg, 1.17 mmol) in CH_2Cl_2 (5 mL) was added triethylamine (177 mg, 0.24 mL, 1.76 mmol) and **2a** (300 mg, 1.17 mmol) at rt. The reaction mixture was stirred for 15 min at room temperature, diluted with Et_2O, and washed with water and brine. The organic layer was dried over $MgSO_4$ and concentrated under reduced pressure. The resulting residue was purified by silica gel column chromatography (AcOEt–*n*-hexane = 1 : 2) to give **5a** (250 mg, 72%) as a yellow oil; IR ν_{max}/cm^{-1} (KBr): 2983, 2857, 1702, 1527, 1469, 1433, 1343, 1283, 1147, 1092, 1076, 1026; ^1H NMR (400 MHz; $CDCl_3$) δ 1.54–164 (6H, m), 3.46 (4H, brs), 5.53 (2H, s), 7.47 (1H, dt, J = 1.5, 8.0 Hz), 7.56 (1H, dd, J = 1.0, 8.0 Hz), 7.64 (1H, dt, J = 1.5, 8.0 Hz), 8.07 (1H, dd, J = 1.0, 8.0 Hz); ^{13}C NMR (75 MHz; DMSO-d_6, 80 °C) δ 23.3, 24.8, 44.1, 62.5, 124.0, 128.5, 128.8, 131.8, 133.2, 147.4, 153.6; Mass (FAB) *m/z* 265 (M + H^+); HRMS (FAB) calcd for $C_{13}H_{17}N_2O_4$: 265.1188. Found: 265.1194.

***N*-1-(2-Nitrophenyl)ethoxycarbonyl piperidine (5b)**

To a solution of piperidine (100 mg, 1.17 mmol) in CH_2Cl_2 (5 mL) was added triethylamine (177 mg, 0.24 mL, 1.76 mmol) and **2d** (360 mg, 1.17 mmol) at rt. The reaction mixture was

stirred for 15 min at room temperature, diluted with Et_2O, and washed with water and brine. The organic layer was dried over $MgSO_4$ and concentrated under reduced pressure. The resulting residue was purified by silica gel column chromatography (AcOEt–*n*-hexane = 1 : 2) to give **5a** (310 mg, 95%) as a yellow oil; IR ν_{max}/cm^{-1} (KBr): 2938, 2857, 1698, 1526, 1468, 1430, 1350, 1283, 1262, 1234, 1147, 1086, 1069, 1023; ^1H NMR (400 MHz; $CDCl_3$) δ: 1.53–1.59 (6H, m), 1.64 (3H, d, J = 6.5 Hz), 3.38–3.47 (4H, m), 6.25 (1H, q, J = 6.5 Hz), 7.38–7.42 (1H, m), 7.58–7.63 (2H, m), 7.91 (1H, dd, J = 1.5, 8.0 Hz); ^{13}C NMR (75 MHz; DMSO-d_6, 80 °C) δ: 21.6, 23.6, 25.2, 44.3, 68.0, 123.8, 127.2 128.5, 133.4, 137.4, 147.7, 153.5; Mass (FAB) *m/z* 279 ($M + H^+$); HRMS (FAB) calcd for $C_{14}H_{19}N_2O_4$: 279.1345. Found: 279.1327.

Relaxation assay of supercoiled plasmid DNA

To a solution of supercoiled pBR 322 DNA (0.15 μg) in pH 7.0 TE buffer (9 μL) was added a DMSO solution of the compounds (1 μL, 10 μM or 100 μM). The reaction mixture was photo-irradiated for 2, 5, 15 or 60 s, and the mixture was incubated for 24 h at 37 °C. The resulting DNA analysis was conducted using electrophoresis (tris-acetate-EDTA buffer, ethidium bromide 1.3 μM solution) on 0.7% native agarose gel at 7.4 v cm^{-1} for 30 min.

Relaxation assay of supercoiled plasmid DNA in the presence of hydroxyl radical or singlet oxygen scavengers

To a solution of supercoiled pBR 322 DNA (0.15 μg) in pH 7.0 TE buffer (9 μL) was added a DMSO solution of the compounds (1 μL, 10 μM or 100 μM) and glycerol (10 mM) or NaN_3 (10 mM). The reaction mixture was photoirradiated for 15 s, and the mixture was incubated for 24 h at 37 °C. The resulting DNA analysis was conducted using electrophoresis (tris-acetate-EDTA buffer, ethidium bromide 1.3 μM solution) on 0.7% native agarose gel at 7.4 V cm^{-1} for 30 min.

Assessment of cytotoxicity of caged DNA alkylating agents toward HepG2 cells under UV irradiation

The human hepatoblastoma cell lines HepG2 were cultured in Dulbecco's modified Eagle's medium (DMEM) containing 4.5 g L^{-1} glucose, supplemented with 10% (v/v) fetal bovine serum (FBS), 100 IU mL^{-1} penicillin and 100 μg mL^{-1} streptomycin. Compounds **3** and **4a–4d** were dissolved in DMSO (100 μM, 1 mM or 10 mM). Each 100 μL of cell suspension was seeded into a 96-well flat-bottomed microplate at a density of 10 000 cells per well and incubated at 37 °C in a 5% CO_2 humidified atmosphere for 24 h. Compound solution (1 μL) was added (for evaluation of membrane permeability, interval times of 0–12 h were used), then UV rays were irradiated for each respective time. After 48 h (for evaluation of membrane permeability, after difference time calculated by interval time to 48 h), 10 μL of MTT solution was added to each well, followed by further incubation for 4 h. 100 μL of 2-propanol was added. The optical densities were observed using a Microplate Reader (BIO-RAD Model 550) at 595 nm.

Acknowledgements

This work was supported in part by a Grant-in-Aid for Science Research from the Japan Society for the Promotion of Science and the Ministry of Education, Culture, Sports, Science and Technology, Japan.

References

1 D. A. Karnofsky, *Ann. N. Y. Acad. Sci.*, 1958, **68**, 899.
2 R. Ralhan and J. Kaur, *Expert Opin. Ther. Pat.*, 2007, **17**, 1061.
3 E. Espinosa, P. Zamora, J. Feliu and M. G. Barón, *Cancer Treat. Rev.*, 2003, **29**, 515.
4 G. Mayer and A. Heckel, *Angew. Chem., Int. Ed.*, 2006, **45**, 4900.
5 I. Saito, M. Takayama and T. Sakurai, *J. Am. Chem. Soc.*, 1994, **116**, 2653.
6 T. C. Judd and R. M. Williams, *Org. Lett.*, 2002, **4**, 3711.
7 K. Haruna, H. Kanezaki, K. Tanabe, W.-M. Dai and S. Nishimoto, *Bioorg. Med. Chem.*, 2006, **14**, 4427.
8 B. Breiner, J. C. Schlatterer, S. V. Kovalenko, N. L. Greenbaum and I. V. Alabgin, *Angew. Chem., Int. Ed.*, 2006, **45**, 3666.
9 B. Breiner, J. C. Schlatterer, I. V. Alabgin, S. V. Kovalenko and N. L. Greenbaum, *Proc. Natl. Acad. Sci. U. S. A.*, 2007, **104**, 13016.
10 W.-Y. Yang, S. Breiner, S. V. Kovalenko, C. Ben, M. Singh, S. N. LeGrand, Q.-X. A. Sang, G. F. Strouse, J. A. Copland and I. V. Alabugin, *J. Am. Chem. Soc.*, 2009, **131**, 11458.
11 R. R. Allison, G. H. Downie, R. Cuenca, X.-H. Hu, C. J. H. Childs and C. H. Sibata, *Photodiagn. Photodyn. Ther.*, 2004, **1**, 27.
12 R. M. Williams, S. B. Rollins and T. C. Judd, *Tetrahedron*, 2000, **56**, 521.
13 S. Park, T. Bndo, K. Shinobara, S. Nishijima and H. Sugiyama, *Bioconjugate Chem.*, 2011, **22**, 120–124.
14 K. Miyashita, M. Park, S. Adachi, S. Seki, S. Obika and T. Imanishi, *Bioorg. Med. Chem. Lett.*, 2002, **12**, 1075.
15 Y. Kawada, T. Kodama, K. Miyashita, T. Imanishi and S. Obika, *Heterocycles*, 2010, **80**, 1249.
16 T. A. Barltrop, P. J. Plant and P. Schofield, *Chem. Commun.*, 1966, 822.
17 J. W. Camberlin, *J. Org. Chem.*, 1966, **31**, 1658.
18 A. Patchornik, B. Amit and R. B. Woodward, *J. Am. Chem. Soc.*, 1970, **92**, 6333.
19 B. Amit, U. Zehavi and A. Patchornik, *J. Org. Chem.*, 1974, **39**, 192.
20 E. Reichmanis, B. C. Smith and R. Gooden, *J. Polym. Sci., Polym. Chem. Ed.*, 1985, **23**, 1.
21 C. G. Bochet, *Tetrahedron Lett.*, 2000, **41**, 6341.
22 A. Hasan, K.-P. Stengele, H. Giegrich, P. Cornwell, K. R. Isham, R. A. Sachleben, W. Pfleiderer and R. S. Foote, *Tetrahedron*, 1997, **53**, 4247.
23 A. L. Simplício, J. M. Clancy and J. F. Gilmer, *Molecules*, 2008, **13**, 519.
24 J. Alexander, R. Cargill, S. R. Michelson and H. Scwam, *J. Med. Chem.*, 1988, **31**, 318.
25 J. Alexander, D. S. Bindra, J. D. Glass, M. A. Holahan, M. L. Renyer, G. S. Rork, G. R. Sitko, M. T. Stranieri, R. F. Stupienski, H. Veerapanane and J. J. Cook, *J. Med. Chem.*, 1996, **39**, 480.
26 D. Kerr, W. Roberts, I. Tebbett and K. Sloan, *Int. J. Pharm.*, 1998, **167**, 37.

Bioorganic & Medicinal Chemistry 20 (2012) 4098–4102

Contents lists available at SciVerse ScienceDirect

Bioorganic & Medicinal Chemistry

journal homepage: www.elsevier.com/locate/bmc

Hybridizing ability and nuclease resistance profile of backbone modified cationic phosphorothioate oligonucleotides

S.M. Abdur Rahman [a,*], Takeshi Baba [b], Tetsuya Kodama [b], Md. Ariful Islam [a], Satoshi Obika [b,*]

[a] Department of Clinical Pharmacy and Pharmacology, Faculty of Pharmacy, University of Dhaka, Dhaka 1000, Bangladesh
[b] Graduate School of Pharmaceutical Sciences, Osaka University, 1-6 Yamadaoka, Suita, Osaka 565-0871, Japan

ARTICLE INFO

Article history:
Received 21 March 2012
Revised 1 May 2012
Accepted 2 May 2012
Available online 12 May 2012

Keywords:
Phosphorothioate
Backbone modification
Aminoalkyl moiety
UV melting experiment
Nuclease resistance

ABSTRACT

Various stereochemically pure cationic phosphorothioate oligonucleotides bearing aminoalkyl moieties were synthesized, and their duplex-forming ability against single-stranded DNA (ssDNA), single-stranded RNA (ssRNA) and triplex-forming ability against double-stranded DNA (dsDNA) were evaluated by UV melting experiments. The cationic *Rp* stereoisomers showed improved duplex-forming ability against ssDNA, triplex-forming ability against dsDNA and nuclease stability.

1. Introduction

Chemically modified oligonucleotides are increasingly used in antisense,[1] antigene,[2] RNA interference (RNAi)[3] and other genomic technologies such as nucleic acid nanotechnology and drug target validation.[4,5] One of the simplest chemical modifications of oligonucleotides is the phosphorothioate (PS) modification in which a non-bridging oxygen on phosphorus is replaced by a sulfur atom.[6] PS oligodeoxynucleotides (ODN) showed great promises in antisense technology because of their ease of synthesis and high resistance to nuclease degradation.[7] The first antisense drug, Vitravene™ (Formivirsen), containing PS-ODN was approved by the FDA in 1998 for the treatment of cytomegalovirus retinitis,[8] and several others are in clinical trials.[9] Derivatives of PS-ODNs have recently been applied in sequence specific DNA cleavage[10] and construction of DNA nanostructures.[11] However, one of the major problems encountered in the use of PS-ODNs is their low hybridizing ability against complementary strands. Duplex-forming ability against ssDNA or ssRNA is reduced gradually[12,13] and triplex-forming ability is greatly diminished or totally lost upon PS modification.[14,15] To overcome these problems, modifications such as introduction of cationic residues, polyamines and stacking enforcers on the nucleobase have been accomplished.[16–21] These strategies improved the duplex-forming ability in many cases; however, triplex-forming ability was either reduced or not determined. Alternatively, mixing of natural and synthetic polyamines of various sizes has also been investigated for improving hybrid stability.[22,23]

Introduction of an additional functional moiety on the backbone to improve the hybridizing ability of ODNs and their nuclease resistance was also investigated.[24] Grafting of cationic functional moieties on the backbone of natural β-ODNs was found to destabilize duplexes/triplexes, whereas grafting with the non-natural α-ODNs was shown to improve the duplex- and triplex-forming abilities.[25] The stabilization of hybrids by cationic moieties lies in their ability to neutralize the repulsive negative charges on the phosphate backbones and generate an electrostatic interaction with the anionic phosphate backbone. Cationic moieties conjugated to ODNs are also known to improve the uptake of ODNs into cells.[26] Among the various modifications engineered on the backbone, most have been performed on the usual phosphodiester linkage and only very few attempts were undertaken to functionalize the sulfur atom of PS-ODN.[10,11,27,28] Labeling of the sulfur atom of PS-ODN was achieved by some groups using alkylating agents containing haloacetamides, aziridine sulfonamides, γ-bromo-α,β-unsaturated carbonyl compounds[27] or malemidyl derivatives.[28] However, incorporation of such groups on the sulfur atom resulted in destabilization of the duplex and no data related to triplex formation has been reported.

The high nuclease resistance of PS-ODN and the lack of sufficient examples of backbone modification prompted us to investigate the conjugation of cationic amino groups on the backbone of PS-ODN. Therefore, we planned to introduce several cationic amino

* Corresponding authors. Tel.: +880 2 9661900 70x8166 (S.M.A.R.); tel.: +81 6 6879 8200; fax: +81 6 6879 8204 (S.O.).
E-mail addresses: rahman_du@yahoo.com (S.M.A. Rahman), obika@phs.osaka-u.ac.jp (S. Obika).

0968-0896/$ - see front matter © 2012 Elsevier Ltd. All rights reserved.
http://dx.doi.org/10.1016/j.bmc.2012.05.009

linkers of different chain lengths to the PS-ODN based on a post-synthetic modification protocol (Scheme 1).[28] Herein, we describe the introduction of various monoamines and diamines of variable lengths onto the PS backbone and their effects on hybridization and nuclease resistance profiles.

2. Results and discussion

2.1. Conjugation of aminoethyl moiety to oligonucleotide containing purine bases

Initially, a 12 mer PS-ODN, 5′-d(GCGTTTsTTTGCT)-3′ (**S1**) containing one phosphorothioate modification at the middle (labeled as s), was used for introducing the 2-aminoethyl group on the sulfur atom according to the reported procedure.[28] The corresponding aminoethyl PS-ODN, 5′-d(GCGTTTs-$_R$TTTGCT)-3′, R = $-CH_2CH_2NH_2$ (**S2**) was obtained, together with a number of cleavage products resulting from alkylation of the guanine residues.[29] The purified diastereoisomeric mixtures of aminoethyl PS-ODN were hybridized with 12 mer complementary ssDNA and ssRNA and the thermal stability or UV melting temperature (T_m) was determined. The thermal stability of the duplex formed with aminoethyl PS-ODN against ssDNA is equal, and that against ssRNA was slightly lower, compared to the T_ms obtained for non-alkylated PS-ODN. The unmodified natural phosphodiester ODN, 5′-d(GCGTTTTT TGCT)-3′ (**S3**) possessed higher T_m than the PS-ODN and aminoethyl PS-ODN.[30]

2.2. Conjugation of aminoalkyl moieties to the polypyrimidine oligonucleotide

Because of the partial formation of cleavage products due to guanine-alkylation and subsequent purification problems, we decided to use a sequence without guanine residue and ultimately selected two separate stereochemically pure *Sp* and *Rp* PS-ODNs 5′-d(CCCTTTsTTTCCT)-3′ (**1*Sp***, **1*Rp***) bearing a polypyrimidine tract.[31] Stereochemistry of the PS-ODNs **1** were determined by comparing the nuclease stability against snake venom phosphodiesterase which cleaves *Rp* isomer faster than *Sp* isomer.[32] A number of monoamines and diamines with variable alkyl chains were conjugated with the stereochemically pure PS-ODNs using the reported protocol[28] and the corresponding aminoalkyl PS derivatives **2*Sp*–10*Sp*** and **2*Rp*–10*Rp*** were obtained in 24–55% yields (Table 1). The aminoalkyl PS-ODNs were purified by RP-HPLC and characterized by MALDI-TOF mass spectrometry (for purification, yield and MALDI-TOF mass data see the Supplementary data).

The synthesized cationic PS-ODNs **2*Sp*–10*Sp*** and **2*Rp*–10*Rp*** were then investigated for their duplex-forming ability against complementary ssDNA and ssRNA targets and the results are compared to the parent PS-ODNs **1*Sp*** and **1*Rp***, respectively (Tables 2 and 3). The T_m of ODNs **1*Sp*** and **1*Rp*** against ssDNA under specified conditions (Table 2) was found to be identical (42 °C). Alkylation by the 2-aminoethyl moiety to the *Sp*- isomer **1*Sp*** (ODN **2*Sp***) decreased the T_m slightly, while that of the *Rp*-isomer (**2*Rp***) increased the T_m by 3 °C. Increasing the aminoalkyl chain length of the *Sp*-isomers, that is introduction of 3-aminopropyl, 4-aminobutyl, 5-aminopentyl and 6-aminohexyl groups (**3*Sp*–6*Sp***) destabilized the duplex to a larger extent than that observed for the short 2-aminoethyl chain (**2*Sp***).

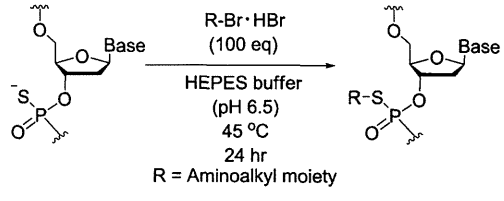

Scheme 1. Conjugation of aminoalkyl groups to phosphorothioate triester.

Table 1
Yields of aminoalkylated phosphorothioate oligonucleotides

Oligonucleotide			Yield (%)	
			Sp	*Rp*
5′-d(CCCTTT$_{s\text{-}R}$TTTCCC)-3′				
R=	H_2N	(**2**)	39	49
	H_2N	(**3**)	41	34
	H_2N	(**4**)	49	42
	H_2N	(**5**)	53	43
	H_2N	(**6**)	44	49
	H_2N N H	(**7**)	24	39
	H_2N N H	(**8**)	28	41
	HN N	(**9**)	55	55
	HN N	(**10**)	33	53

Cationization of **1*Sp*** by acyclic and cyclic diamino moieties (**7*Sp*–10*Sp***) also destabilized the duplex and the corresponding *Rp*-ODNs (**7*Rp*–10*Rp***) exhibited enhanced duplex stability (T_m increased by 3 °C). For most of the *Rp* conjugates, thermal stability was equal to or slightly improved than that of the natural phosphodiester ODN **11**. Melting temperatures in the absence of salt (NaCl) were also recorded for **2*Sp***, **2*Rp*** and **9*Sp***, **9*Rp*** and the results were compared to those obtained for **1*Sp*** and **1*Rp***. The ΔT_m of both **2*Rp*** and **9*Rp*** compared to **1*Rp*** was found to be +3 °C and that for the *Sp*-isomers **2*Sp*** and **9*Sp*** was −2 °C compared to **1*Sp*** (data not shown). Therefore, the increase and the decrease of T_m in the absence or presence of NaCl were similar, indicating that these changes of T_ms are related to the structure of the ODNs. The increase of T_m against ssDNA using *Rp*-ODNs might be very interesting for constructing recently reported protein based nanostructures[11] or for designing amino modified ODN probes for DNA microarrays.[33] The difference of T_m between *Sp*- and *Rp*-isomers is significant; for example for **7*Rp*** and **7*Sp*** the difference is 5 °C by a single modification. Anionic sulfur atoms of *Sp*- and *Rp*-ODNs are faced to the inside and the outside of the duplex, respectively. Inward orientation is expected to cause a negative charge repulsion between anionic sulfur atom and negative charge present in complementary strand.[34] Aminoalkylation neutralizes negative charge at the sulfur atom and decreases the unfavorable repulsion. This neutralization effect stabilized duplexes formed with the *Rp*-ODNs whereas the stabilization effect might be weak in case of outward-oriented *Sp*-ODNs.

Against the complementary ssRNA (Table 3), all aminoalkyl functional *Sp* PS-ODNs (**2*Sp*–10*Sp***) showed decreased T_m compared to the parent ODN **1*Sp***. *Rp*-isomers (**2*Rp*–10*Rp***) also afforded slightly decreased or equal T_m. These results show that irrespective of the stereoisomers, modification of a sulfur atom on a phosphorothioate linkage by an aminoalkyl moiety usually is detrimental for A-form DNA/RNA duplex stability and destabilization is more pronounced in duplexes formed by *Sp*-conformers. This destabilization effect may result from an unfavorable steric interaction or disturbance of the hydration pattern found in A-form duplexes.[35]

Table 2
Thermal stability of duplexes formed by cationic *Sp* and *Rp* isomers with complementary ssDNA[a,b]

Oligonucleotide		*Sp*		*Rp*	
		T_m[c]	ΔT_m	T_m[c]	ΔT_m
5′-d(CCCTTT$_s$TTTCCC)-3′ 5′-d(CCCTTT$_{s\text{-}R}$TTTCCC)-3′	(**1**)	42	–	42	–
R= H_2N	(**2**)	41	−1	45	+3
H_2N	(**3**)	40	−2	43	+1
H_2N	(**4**)	40	−2	44	+2
H_2N	(**5**)	39	−3	44	+2
H_2N	(**6**)	37	−5	42	0
H_2N, N, H	(**7**)	40	−2	45	+3
H_2N, N, H	(**8**)	40	−2	45	+3
HN, N	(**9**)	40	−2	45	+3
HN, N	(**10**)	41	−1	45	+3

[a] Target ssDNA: 5′-d(AGGAAAAAAGGG)-3′.
[b] T_m values of the natural oligonucleotide 5′-d(CCCTTTTTTCCT)-3′ (**11**) for ssDNA is 44 °C.
[c] T_m condition: 10 mM sodium phosphate buffer (pH 7.2), 100 mM NaCl, 4 μM each oligonucleotide.

Table 3
Thermal stability of duplexes formed by cationic *Sp* and *Rp* isomers with complementary ssRNA[a,b]

Oligonucleotide		*Sp*		*Rp*	
		T_m[c]	ΔT_m	T_m[c]	ΔT_m
5′-d(CCCTTT$_s$TTTCCC)-3′ 5′-d(CCCTTT$_{s\text{-}R}$TTTCCC)-3′	(**1**)	46	–	46	–
R= H_2N	(**2**)	43	−3	45	−1
H_2N	(**3**)	43	−3	46	0
H_2N	(**4**)	43	−3	45	−1
H_2N	(**5**)	42	−4	44	−2
H_2N	(**6**)	41	−5	43	−3
H_2N, N, H	(**7**)	44	−2	45	−1
H_2N, N, H	(**8**)	44	−2	46	0
HN, N	(**9**)	44	−2	46	0
HN, N	(**10**)	43	−3	45	−1

[a] Target ssRNA: 5′-r(AGGAAAAAAGGG)-3′.
[b] T_m values of the natural oligonucleotide 5′-d(CCCTTTTTTCCT)-3′ (**11**) for ssRNA is 48 °C.
[c] T_m condition: 10 mM sodium phosphate buffer (pH 7.2), 100 mM NaCl, 4 μM each oligonucleotide.

It is possible that the cationic *Rp*-isomers enhanced the stability of B-form DNA/DNA duplexes while destabilizing the A-form DNA/RNA duplex due to the fact that in the case of the A-form duplex, long lived hydration patterns are present in the deep major groove and involve a sequence independent water bridge between the *pro*Rp oxygen atom and the adjacent phosphate group,[36] whereas such interactions are absent in B-form duplexes because the corresponding distance is too long.[37]

Next, we investigated the triplex formation at pH 5.5 towards 22-bp dsDNA target bearing a homopurine–homopyrimidine tract. The same ODNs used in duplex studies were employed for the triplex study and the results are summarized in Table 4. All the aminoalkyl conjugates of the *Sp*-isomer caused destabilization of the triplex as shown by the ΔT_m values. In remarkable contrast, all aminoalkyl *Rp*-conformers increased the T_m values with respect to that obtained for **1*Rp***. The increase of T_m varies depending on the size and structural features of the aminoalkyl substituents and the highest increase of T_m (ΔT_m = +6 °C) was noted for ODN **8*Rp*** consisting of a 2-(3-aminopropyl)aminoethyl moiety. Another notable increase of T_m was found for the diamine derivative **7*Rp*** (ΔT_m = +5 °C) bearing the 2-(2-aminoethyl)aminoethyl moiety. The increase of T_ms using **7*Rp*** and **8*Rp*** is also greater than that

Table 4
Thermal stability of triplexes formed by cationic *Sp* and *Rp* isomers with complementary dsDNA[a,b]

Oligonucleotide			*Sp*		*Rp*	
			T_m[c]	ΔT_m	T_m[c]	ΔT_m
5′-d(CCCTTT$_5$TTTCCC)-3′ 5′-d(CCCTTT$_{5\text{-}R}$TTTCCC)-3′		(**1**)	26	–	25	–
R=	H_2N	(**2**)	24	−2	29	+4
	H_2N	(**3**)	24	−2	29	+4
	H_2N	(**4**)	24	−2	27	+2
	H_2N	(**5**)	24	−2	27	+2
	H_2N	(**6**)	23	−3	27	+2
	H_2N N H	(**7**)	25	−1	30	+5
	H_2N N H	(**8**)	25	−1	31	+6
	HN N	(**9**)	24	−2	28	+3
	HN N	(**10**)	23	−3	27	+2

[a] Target dsDNA: 5′-d(GCAGCGGGAAAAAAGGAGCAGC)-3′/3′- d(CGTCGCCCTTTTTTCCTCGTCG)-5′.
[b] T_m values of the natural oligonucleotide 5′-d(CCCTTTTTTCCT)-3′ (**11**) for dsDNA is 29 °C.
[c] T_m condition: 7 mM sodium phosphate buffer (pH 5.5), 140 mM KCl, 10 mM $MgCl_2$, 1.5 μM Oligonucleotide.

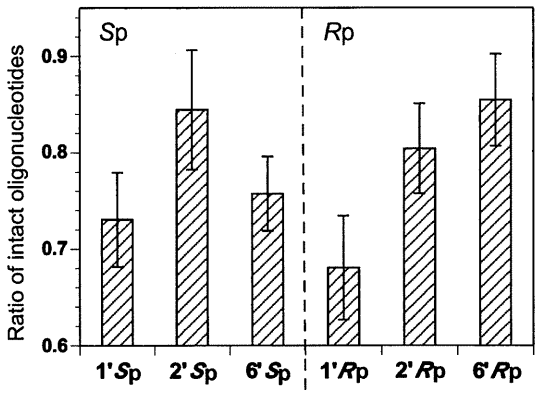

Figure 1. Enzymatic stability of 5′-d(CCCTTTsT)-3′ (**1′*Sp*, 1′*Rp***) and 5′-d(CCCTTTs-$_R$T)-3′ (**2′*Sp*, 2′*Rp*** and **6′*Sp*, 6′*Rp***) against *Crotalus Admanteus* Venom Phosphodiesterase (CAVP). Experiments were carried out at 37 °C for 15 min in buffer containing 50 mM Tris–HCl (pH 7.5), 10 mM $MgCl_2$, each ODNs and CAVP.

observed for natural unmodified phosphodiester ODN **11**. The T_m observed for **8*Rp*** was 2 °C higher than that obtained for the natural phosphodiester ODN **11**. This increase of T_m by the *Rp* congeners might arise from neutralization of the repulsive forces in the phosphate backbone via cationization of the third strand or via favorable intra or interstrand interaction between positively charged amino groups and phosphate oxygens, similar to that obtained using polyamines.[38]

Triplex formation using phosphorothioate ODN is inefficient in most cases and usually a large decrease of T_m is observed upon PS modification, which restricts the use of PS-ODN in antigene technology.[14,15] However, the incremental increase of T_m by 4 or 5 °C by single 3-(2-aminoethyl)aminoethyl or 2-(2-aminopropyl)aminoethyl linked PS-ODN implies that cationic PS-ODNs might be interesting candidates for antigene technology. This property along with the increased T_m over natural unmodified ODN might be very interesting for designing triplex-forming oligonucleotides (TFO) for antigene technologies and recently reported site specific DNA cleavage using PS-TFO.[10]

2.3. Evaluation of nuclease stability of the conjugated oligonucleotides

Conjugation of a functional moiety to the sulfur atom of PS-ODN is effective in improving the nuclease resistance property.[10] We evaluated the nuclease stability of aminoalkylated PS-ODN using 3′-exo nuclease [*Crotalus Admanteus* Venom Phosphodiesterase (CAVP)]. First, we attempted to investigate the stability of ODN **8*Rp***, which showed the highest triplex-forming ability, and its diastereomer **8*Sp***. However, unexpectedly, **8*Rp*** and **8*Sp*** were heat-labile. Therefore, **8*Sp***, **8*Rp*** were substituted for **2*Sp***, **2*Rp*** and **6*Sp***, **6*Rp*** bearing amino moieties at the same position as **8*Sp***, **8*Rp***. For easier comparison of the nuclease stability of aminoalkylated PS-ODNs, 12 mer ODNs were digested from the 3′-position in advance to give 7 mer ODNs, 5′-d(CCCTTTsT)-3′ (**1′*Sp***, **1′*Rp***), 5′-d(CCCTTTs-$_R$T)-3′ (R = $-(CH_2)_2NH_2$, **2′*Sp***, **2′*Rp***), (R = $-(CH_2)_6NH_2$, **6′*Sp***, **6′*Rp***). The resulting ODNs were incubated with CAVP once again and the ratio of the remaining ODNs at 15 min was evaluated (Fig. 1). The *Sp* PS-ODN **1′*Sp*** showed slightly higher stability than *Rp* PS-ODN **1′*Rp***. The aminoalkylated *Sp* PS-ODNs (**2′*Sp*, 6′*Sp***) showed comparable or higher nuclease stability than **1′*Sp***. In contrast, aminoalkylated *Rp* PS-ODN (**2′*Rp*, 6′*Rp***) showed further enhanced nuclease stability compared to **1′*Rp***. Interestingly, the stability of the *Rp* and *Sp* isomers was reversed by conjugation of an aminohexyl moiety. Aminoalkylation on the sulfur atom is effective to improve the nuclease stability of PS-ODN, notably *Rp*-isomers.

3. Conclusion

In conclusion, we have successfully introduced various aminoalkyl moieties to the sulfur group of stereodefined PS-ODNs. The aminoalkyl conjugated *Rp*-isomers of phosphorothioate exhibited increased stabilization of DNA duplexes while the *Sp*-conformers destabilized the duplexes. Both the cationic *Rp*- and *Sp*-isomers showed decreased affinity towards RNA. Triplex formation was enhanced by all the aminoalkyl functionalized *Rp*-isomers. The most significant triplex stabilization was observed with 2-(3-aminopropyl)aminoethyl and 2-(2-aminoethyl)aminoethyl linked *Rp*-PS-ODNs. We also revealed that the alkylation of PS-ODNs is effective to enhance the nuclease stability and increase of nuclease stability

is more pronounced for *Rp* isomers. Considering all the results we assume that cationic *Rp*-PS-ODNs might be an interesting candidate for DNA based technologies such as DNA microarray, DNA nanostructures and antigene technologies.

4. Experimental section

4.1. General information

Melting points are uncorrected. ^{1}H NMR (400 MHz) and ^{13}C NMR (100 MHz) were recorded on a JEOL JNM-ECS-400 spectrometer. Chemical shifts are reported in parts per million downfield from residual solvent of D_2O (4.79 ppm) for ^{1}H NMR or methanol-d_4 (49.0 ppm) for ^{13}C NMR. Mass spectra were measured on JEOL JMS-700 mass spectrometers. MALDI-TOF mass spectra were recorded on a Bruker Daltonics Autoflex II TOF/TOF mass spectrometer. For high performance liquid chromatography (HPLC), Shimadzu LC-10AT$_{VP}$, SPD-10A$_{VP}$ and CTO-10$_{VP}$ were used. Thermal denaturation experiments were carried out on Shimadzu UV-1650 and UV-1800 spectrophotometers equipped with a T_m analysis accessory. Oligonucleotide **1** was purchased from GeneDesign Inc. Aminoalkylating reagents were purchased (ethyl and propyl) or synthesized (others except for 6-bromohexylammonium bromide)[39–41] as the respective ammonium bromides.

4.2. Synthesis of 6-bromohexylammonium bromide

6-Aminohexanol (500 mg, 4.27 mmol) was slowly added to a stirring 48% hydrogen bromide solution (5.1 mL) at 0 °C and the resulting mixture was stirred at 80 °C for 20 h. The mixture was concentrated and crystallized from toluene/ethanol = 50/1 to give 6-bromohexylammonium bromide (674 mg, 2.6 mmol, 61%) as a white solid.

Mp 130–133 °C (toluene/ethanol = 50/1). ^{1}H NMR (400 MHz, D_2O): δ 1.37–1.48 (4H, m), 1.61–1.68 (2H, m), 1.82–1.87 (2H, m), 2.96 (2H, t, J = 8 Hz), 3.48 (2H, t, J = 7 Hz). ^{13}C NMR (100 MHz, CD_3OD): δ 26.6, 28.4, 28.6, 33.6, 34.2, 40.6. MS (FAB) *m/z* 180 ($M-Br^-$). HRMS (FAB): Calcd for $C_6H_{15}NBr$ ($M-Br^-$): 180.0382. Found: 180.0395.

4.3. Synthesis of aminoalkylated PS-ODNs

Each aminoalkylation reagent (1.0 M, 2 μL, 2 μmol) in DMF (for ODN **2**–**6**) or H_2O (for ODN **7**–**10**) was added to a solution of ODN **1** (10 nmol) in 22 mM HEPES buffer (18 μL, pH 6.5) and the reaction mixture was incubated at 45 °C for 24 h. After completing the reaction, ODN was precipitated by adding ethanol (100 μL). The mixture was kept at 0 °C for 15 min, centrifuged at 13,200 rpm for 15 min at 4 °C, and the resulting supernatant solution was removed. The obtained ODN was purified by RP-HPLC and characterized by MALDI-TOF mass spectrometry.

4.4. Preparation of enzymatically digested ODNs

Crotalus Admanteus Venom Phosphodiesterase (CAVP, Pharmacia Biotech) (1.3 μg for **1′** and **6′*Rp***, 4.5 μg for **2′*Sp***, 4.1 μg for **2′*Rp***, 1.3 μg for **6′*Sp***) was added to a solution of 3.3 μM ODN (5.0 nmol for **1′** and **6′*R***, 4.5 nmol for **2′*Sp***, 4.1 nmol for **2′*Rp***, 5.1 nmol for **6′*Sp***) in 25 mM Tris–HCl buffer (pH 8.5 for **1′**, **6′**, pH 7.5 for **2′**) containing 4.0 mM $MgCl_2$. The reaction mixture was incubated at 37 °C for 30 min and heated to 90 °C for 30 min to inactivate the nuclease. The mixture was concentrated and purified by RP-HPLC.

4.5. Evaluation of nuclease stability

Crotalus Admanteus Venom Phosphodiesterase (CAVP, Pharmacia Biotech) (0.40 μg) was added to a solution of 3.3 μM ODN (0.40 nmol) in 50 mM Tris–HCl buffer (pH 7.5) containing 10 mM $MgCl_2$. The reaction mixture was incubated at 37 °C for 15 min and heated to 90 °C for 5 min to inactivate the nuclease. The amount of intact ODN was quantified by HPLC.

Acknowledgments

A part of this work was supported by the bilateral joint projects conducted by Japan Society of Promotion of Science (JSPS) and University Grants Commission of Bangladesh (UGC)

Supplementary data

Supplementary data associated with this article can be found, in the online version, at http://dx.doi.org/10.1016/j.bmc.2012.05.009.

References and notes

1. Crooke, S. T. *Annu. Rev. Med.* **2004**, *55*, 61.
2. Buchini, S.; Leumann, C. J. *Curr. Opin. Chem. Biol.* **2003**, *7*, 717.
3. Novina, C. D.; Sharp, P. A. *Nature* **2004**, *430*, 161.
4. Yan, H. *Science* **2004**, *306*, 2048.
5. Taylor, M. F.; Wiederholt, K.; Sverdrup, F. *Drug Discovery Today* **1999**, *4*, 562.
6. Stein, C. A.; Cheng, Y.-C. *Science* **1993**, *261*, 1004.
7. Eckstein, F. *Annu. Rev. Biochem.* **1985**, *54*, 367.
8. Marwick, C. *J. Am. Med. Assoc.* **1998**, *280*, 871.
9. Yamamoto, T.; Nakatani, M.; Narukawa, K.; Obika, S. *Future Med. Chem.* **2011**, *3*, 339.
10. Vekhoff, P.; Halby, L.; Oussedik, K.; Dallavalle, S.; Merlini, L.; Mahieu, C.; Lansiaux, A.; Bailly, C.; Boutorine, A.; Pisano, C.; Giannini, G.; Alloatti, D.; Arimondo, P. B. *Bioconjugate Chem.* **2009**, *20*, 666.
11. Lee, J. H.; Wong, N. Y.; Tan, L. H.; Wang, Z.; Lu, Y. *J. Am. Chem. Soc.* **2010**, *132*, 8906.
12. Stein, C. A.; Subasinghe, C.; Shinozuka, K.; Cohen, J. S. *Nucleic Acids Res.* **1988**, *16*, 3209.
13. Clark, C. L.; Cecil, P. K.; Singh, D.; Gray, D. M. *Nucleic Acids Res.* **1997**, *25*, 4098.
14. Xodo, L.; Alunni-Fabbroni, M.; Manzini, G.; Quadrifoglio, F. *Nucleic Acids Res.* **1994**, *22*, 3322.
15. Kim, S.-G.; Tsukahara, S.; Yokoyama, S.; Takaku, H. *FEBS. Lett.* **1992**, *314*, 29.
16. Haginoya, N.; Ono, A.; Nomura, Y.; Ueno, Y.; Matsuda, A. *Bioconjugate Chem.* **1997**, *8*, 271.
17. Ueno, Y.; Mikawa, M.; Matsuda, A. *Bioconjugate Chem.* **1998**, *9*, 33.
18. Matsukura, M.; Okamoto, T.; Miike, T.; Sawai, H.; Shinozuka, K. *Biochem. Biophys. Res. Commun.* **2002**, *293*, 1341.
19. Moriguchi, T.; Sakai, H.; Suzuki, H.; Shinozuka, K. *Chem. Pharm. Bull.* **2008**, *56*, 1259.
20. Lin, K.-Y.; Jones, R. J.; Matteucci, M. *J. Am. Chem. Soc.* **1995**, *117*, 3873.
21. Lin, K.-Y.; Matteucci, M. D. *J. Am. Chem. Soc.* **1998**, *120*, 8531.
22. Venkiteswaran, S.; Vijayanathan, V.; Shirahata, A.; Thomas, T.; Thomas, T. J. *Biochemistry* **2005**, *44*, 303.
23. Winkler, J.; Saadat, K.; Díaz-Gavilán, M.; Urban, E.; Noe, C. R. *Eur. J. Med. Chem.* **2009**, *44*, 670.
24. Morvan, F.; Debart, F.; Vasseur, J.-J. *Chem. Biodivers.* **2010**, *7*, 494.
25. Michel, T.; Debart, F.; Heitz, F.; Vasseur, J.-J. *ChemBioChem* **2005**, *6*, 1254.
26. Fraley, A. W.; Pons, B.; Dalkara, D.; Nullans, G.; Behr, J.-P.; Zuber, G. *J. Am. Chem. Soc.* **2006**, *128*, 10763.
27. Fidanza, J. A.; Ozaki, H.; McLaughlin, L. W. *J. Am. Chem. Soc.* **1992**, *114*, 5509.
28. Chen, M.; Gothelf, K. V. *Org. Biomol. Chem.* **2008**, *6*, 908.
29. The cleavage products were characterized by MALDI-TOF mass data. The alkylation may occur at N7 of guanine residue resulting in cleavage of sugar-base bond.
30. The T_m values of the ODNs were summarized in ESI.
31. The polypyrimidine ODN was selected so that it also can be used both for duplex and triplex studies.
32. Burgers, P. M. J.; Eckstein, F. *Biochemistry* **1979**, *18*, 592.
33. Kamisetty, N. K.; Pack, S. P.; Nonogawa, M.; Devarayapalli, K. C.; Watanabe, S.; Kodaki, T.; Makino, K. *Anal. Bioanal. Chem.* **2007**, *387*, 2027.
34. Jaroszewski, J. W.; Syi, J.-L.; Maizel, J.; Cohen, J. S. *Anti-Cancer Drug Des.* **1992**, *7*, 253.
35. Egli, M.; Portmann, S.; Usman, N. *Biochemistry* **1996**, *35*, 8489.
36. Sundaralingam, M.; Pan, B. *Biophys. Chem.* **2002**, *95*, 273.
37. Egli, M.; Tereshko, V.; Teplova, M.; Minasov, G.; Joachimiak, A.; Sanishvili, R.; Weeks, C. M.; Miller, R.; Maier, M. A.; An, H.; Cook, D. P.; Manoharan, M. *Biopolymers* **1998**, *48*, 234.
38. Ouameur, A. A.; Tajmir-Riahi, H-A. *J. Biol. Chem.* **2004**, *279*, 42041.
39. Hedrera, M. E.; Perillo, I. A. *J. Heterocycl. Chem.* **2000**, *37*, 1431.
40. Piper, J. R.; Stringfellow, C. R., Jr.; Elliott, R. D.; Johnston, T. P. *J. Med. Chem.* **1969**, *12*, 236.
41. McElvain, S. M.; Bannister, L. W. *J. Am. Chem. Soc.* **1954**, *76*, 1126.